



MID-AMERICA TRANSPORTATION CENTER

Report # MATC-UNL: 057

Final Report
WBS:25-1121-0003-057

UNIVERSITY OF
Nebraska
Lincoln

K-STATE
Kansas State University

KU
THE UNIVERSITY OF
KANSAS

MISSOURI
S&T
University of
Science & Technology

**UNIVERSITY OF
LINCOLN**
University

 University of Missouri

IOWA STATE
UNIVERSITY


THE UNIVERSITY OF IOWA

Performance Characteristics of Posts Embedded in Soil

Brandt M. Humphrey, B.S.C.E., E.I.T.

Graduate Research Assistant
Midwest Roadside Safety Facility (MwRSF)
University of Nebraska-Lincoln

Karla A. Lechtenberg, M.S.M.E., E.I.T.

Research Associate Engineer, MwRSF

John D. Reid, Ph.D.

Professor, University of Nebraska-Lincoln

Ronald K. Faller, Ph.D., P.E.

Director, Research Assistant Professor, MwRSF

James C. Holloway, M.S.C.E., E.I.T.

Test Site Manager, MwRSF

UNIVERSITY OF
Nebraska
Lincoln

2015

A Cooperative Research Project sponsored by
U.S. Department of Transportation-Research
and Innovative Technology Administration

The contents of this report reflect the views of the authors, who are responsible for the facts and the accuracy of the information presented herein. This document is disseminated under the sponsorship of the Department of Transportation University Transportation Centers Program, in the interest of information exchange.
The U.S. Government assumes no liability for the contents or use thereof.

MATC



TESTING CERT # 2937.01

MATC Research Project Number 25-1121-0003-057

NDOR Research Project Number SPR-P1(13)M326

PERFORMANCE CHARACTERISTICS OF POSTS EMBEDDED IN SOIL

Submitted by

Brandt M. Humphrey, B.S.C.E., E.I.T.
Graduate Research Assistant

Karla A. Lechtenberg, M.S.M.E., E.I.T.
Research Associate Engineer

John D. Reid, Ph.D.
Professor

Ronald K. Faller, Ph.D., P.E.
Research Assistant Professor
MwRSF Director

James C. Holloway, M.S.C.E., E.I.T.
Test Site Manager

MIDWEST ROADSIDE SAFETY FACILITY

Nebraska Transportation Center
University of Nebraska-Lincoln
130 Whittier Research Center
2200 Vine Street
Lincoln, Nebraska 68583-0853
(402) 472-0965

Submitted to

Nebraska Department of Roads
1500 Nebraska Highway 2
Lincoln, Nebraska 68502

Mid-America Transportation Center
U.S. Department of Transportation
Region VII University Transportation Center
University of Nebraska-Lincoln
2200 Vine Street, 262 Whittier Building
Lincoln, Nebraska 68583-0853

MwRSF Research Report No. TRP-03-301-15

August 12, 2015

TECHNICAL REPORT DOCUMENTATION PAGE

1. Report No. TRP-03-301-15	2.	3. Recipient's Accession No.	
4. Title and Subtitle Performance Characteristics of Posts Embedded in Soil		5. Report Date August 12, 2015	
7. Author(s) Humphrey, B.M., Lechtenberg, K.A., Reid, J.D., Faller, R.K., and Holloway, J.C.		8. Performing Organization Report No. TRP-03-301-15	
9. Performing Organization Name and Address Midwest Roadside Safety Facility (MwRSF) Nebraska Transportation Center University of Nebraska-Lincoln 130 Whittier Research Center 2200 Vine Street Lincoln, Nebraska 68583-0853		10. Project/Task/Work Unit No.	
12. Sponsoring Organization Name and Address Nebraska Department of Roads (NDOR) 1500 Nebraska Highway 2 Lincoln, Nebraska 68502 Mid-America Transportation Center (MATC) U.S. Department of Transportation Region VII University Transportation Center University of Nebraska-Lincoln 113 Nebraska Hall Lincoln, Nebraska 68588-0530		11. Contract © or Grant (G) No. MATC No. 25-1121-0003-057 NDOR No. SPR-P1(13)M326	
15. Supplementary Notes Prepared in cooperation with U.S. Department of Transportation, Federal Highway Administration.		13. Type of Report and Period Covered Final Report: 2012 – 2015	
16. Abstract (Limit: 200 words) The primary objective of this research study was to determine the post-soil impact reaction of W6x8.5 (W150x12.6) steel posts and 6-in. x 8-in. (152-mm x 203-mm) Southern Yellow Pine (SYP) posts, specifically along the weak axis. Five bogie tests were conducted on W6x8.5 (W150x12.6) A992 steel posts with a length of 72 in. with embedment depths ranging between of 24 and 40 in. (610 and 1,016 mm). Four bogies tests were conducted on 6-in. x 8-in. (152 mm x 203 mm) SYP posts embedded at depths ranging between 30 and 40 in. (735 and 1,016 mm). The target impact conditions were an impact speed of 20 mph (32.2 km/h) and an impact angle of 0 degrees creating weak-axis bending. The posts were impacted 24 7/8 in. (632 mm) above the groundline and perpendicular to the web of the post. A compacted, coarse crushed limestone material as recommended by the Manual for Assessing Safety Hardware (MASH) was utilized for all tests. For each test, acceleration data was used to determine force vs. displacement and energy vs. displacement and failure mechanisms of the post-soil system were noted. Conclusions and recommendations were made that pertain to the embedment depth of posts impacted along the weak axis.		14. Sponsoring Agency Code	
17. Document Analysis/Descriptors Highway Safety, Crash Test, Roadside Appurtenances, Compliance Test, MASH, Steel Post, Southern Yellow Pine, SYP, Weak Axis, Impact Testing		18. Availability Statement No restrictions. Document available from: National Technical Information Services, Springfield, Virginia 22161	
19. Security Class (this report) Unclassified	20. Security Class (this page) Unclassified	21. No. of Pages 68	22. Price

DISCLAIMER STATEMENT

This report was completed with funding in part from the Federal Highway Administration, U.S. Department of Transportation (USDOT). The contents of this report reflect the views and opinions of the authors who are responsible for the facts and the accuracy of the data presented herein. The contents do not necessarily reflect the official views or policies of the Mid-America Transportation Center (MATC) or the Federal Highway Administration (FHWA), U.S. Department of Transportation. This report does not constitute a standard, specification, regulation, product endorsement, or an endorsement of manufacturers.

UNCERTAINTY OF MEASUREMENT STATEMENT

The Midwest Roadside Safety Facility (MwRSF) has determined the uncertainty of measurements for several parameters involved in standard full-scale crash testing and non-standard testing of roadside safety features. Information regarding the uncertainty of measurements for critical parameters is available upon request by the sponsor and the Federal Highway Administration.

INDEPENDENT APPROVING AUTHORITY

The Independent Approving Authority (IAA) for the data contained herein was Mr. Scott Rosenbaugh, M.S.C.E., E.I.T.

ACKNOWLEDGEMENTS

The authors wish to acknowledge several sources that made a contribution to this project:

(1) the Mid-America Transportation Center, (2) the Federal Highway Administration, U.S. Department of Transportation, and (3) MwRSF personnel for constructing the barriers and conducting the crash tests.

Acknowledgement is also given to the following individuals who made a contribution to the completion of this research project.

Midwest Roadside Safety Facility

J.C. Holloway, M.S.C.E., E.I.T., Test Site Manager
R.W. Bielenberg, M.S.M.E., E.I.T., Research Associate Engineer
S.K. Rosenbaugh, M.S.C.E., E.I.T., Research Associate Engineer
J.D. Schmidt, Ph.D., P.E., Research Assistant Professor
C.S. Stolle, Ph.D., Research Assistant Professor
A.T. Russell, B.S.B.A., Shop Manager
K.L. Krenk, B.S.M.A., Maintenance Mechanic (retired)
S.M. Tighe, Laboratory Mechanic
D.S. Charroin, Laboratory Mechanic
M.A. Rasmussen, Laboratory Mechanic
E.W. Krier, Laboratory Mechanic
Undergraduate and Graduate Research Assistants

Nebraska Department of Roads

Phil TenHulzen, P.E., Design Standards Engineer
Jim Knott, P.E., State Roadway Design Engineer
Jodi Gibson, Research Coordinator

Federal Highway Administration

John Perry, P.E., Nebraska Division Office
Danny Briggs, Nebraska Division Office

TABLE OF CONTENTS

TECHNICAL REPORT DOCUMENTATION PAGE i

DISCLAIMER STATEMENT ii

UNCERTAINTY OF MEASUREMENT STATEMENT ii

INDEPENDENT APPROVING AUTHORITY..... ii

ACKNOWLEDGEMENTS iii

TABLE OF CONTENTS..... iv

LIST OF FIGURES vi

LIST OF TABLES viii

1 INTRODUCTION 1

 1.1 Background 1

 1.2 Objective 1

 1.3 Scope..... 1

2 TEST CONDITIONS..... 2

 2.1 Test Facility 2

 2.2 Equipment and Instrumentation..... 2

 2.2.1 Bogie 2

 2.2.2 Accelerometers 3

 2.2.3 Retroreflective Optic Speed Trap 3

 2.2.4 Digital Photography 4

 2.3 End-of-Test Determination 4

 2.4 Data Processing..... 5

3 COMPONENT TESTING RESULTS AND DISCUSSION 6

 3.1 Purpose..... 6

 3.2 Scope..... 6

 3.3 Results..... 11

 3.3.1 Test No. WAP-1..... 11

 3.3.2 Test No. WAP-2..... 14

 3.3.3 Test No. WAP-3..... 16

 3.3.4 Test No. WAP-4..... 18

 3.3.5 Test No. WAP-5..... 20

 3.3.1 Test No. SYPW-1 22

 3.3.2 Test No. SYPW-2 24

 3.3.3 Test No. SYPW-3 26

 3.3.4 Test No. SYPW-4 28

 3.4 Discussion..... 30

 3.4.1 Steel Posts (Test Nos. WAP-1 through WAP-5) 30

3.4.2 Wood Posts (SYPW-1 through SYPW-4) 35

4 SUMMARY, CONCLUSIONS, AND RECOMMENDATIONS 39

5 REFERENCES 42

6 APPENDICES 43

 Appendix A. Material Specifications 44

 Appendix B. Bogie Test Results 50

 Appendix C. SYP Post Inspection..... 65

LIST OF FIGURES

Figure 1. Rigid-Frame Bogie on Guidance Track	3
Figure 2. Bogie Test Matrix and Setup, W6x8.5 (W150x12.6) Steel Posts	7
Figure 3. Weak-Axis Impact Post Details, W6x8.5 (W150x12.6) Steel Posts	8
Figure 4. Bogie Test Matrix and Setup, 6-in. x 8-in. (152-mm x 203-mm) SYP Posts	9
Figure 5. Weak-Axis Impact Post Details, 6-in. x 8-in. (152-mm x 203-mm). SYP Posts	10
Figure 6. Force vs. Deflection and Energy vs. Deflection, Test No. WAP-1	12
Figure 7. Time-Sequential and Post-Impact Photographs, Test No. WAP-1	13
Figure 8. Force vs. Deflection and Energy vs. Deflection, Test No. WAP-2	14
Figure 9. Time-Sequential and Post-Impact Photographs, Test No. WAP-2	15
Figure 10. Force vs. Deflection and Energy vs. Deflection, Test No. WAP-3	16
Figure 11. Time-Sequential and Post-Impact Photographs, Test No. WAP-3	17
Figure 12. Force vs. Deflection and Energy vs. Deflection, Test No. WAP-4	18
Figure 13. Time-Sequential and Post-Impact Photographs, Test No. WAP-4	19
Figure 14. Force vs. Deflection and Energy vs. Deflection, Test No. WAP-5	20
Figure 15. Time-Sequential and Post-Impact Photographs, Test No. WAP-5	21
Figure 16. Force vs. Deflection and Energy vs. Deflection, Test No. SYPW-1	22
Figure 17. Time-Sequential and Post-Impact Photographs, Test No. SYPW-1	23
Figure 18. Force vs. Deflection and Energy vs. Deflection, Test No. SYPW-2	24
Figure 19. Time-Sequential and Post-Impact Photographs, Test No. SYPW-2	25
Figure 20. Force vs. Deflection and Energy vs. Deflection, Test No. SYPW-3	26
Figure 21. Time-Sequential and Post-Impact Photographs, Test No. SYPW-3	27
Figure 22. Force vs. Deflection and Energy vs. Deflection, Test No. SYPW-4	28
Figure 23. Time-Sequential and Post-Impact Photographs, Test No. SYPW-4	29
Figure 24. Force vs. Deflection Comparison, WAP-1 through WAP-5	33
Figure 25. Energy vs. Deflection Comparison, Test Nos. WAP-1 through WAP-5	34
Figure 26. Comparison of Post Fractures, Test Nos. SYPW-1 (Left) and SYPW-4 (Right)	36
Figure 27. Force vs. Deflection Comparison, Test Nos. SYPW-1 through SYPW-4	37
Figure 28. Energy vs. Deflection Comparison, Test Nos. SYPW-1 through SYPW-4	38
Figure 29. Combined Force vs. Deflection Comparison, All Bogie Tests	40
Figure 30. Combined Energy vs. Deflection Comparison, All Bogie Tests	41
Figure A-1. Material Specifications, W6x8.5 (W150x12.6) Steel Post, Test Nos. WAP-1 through WAP-5	45
Figure A-2. Material Specifications, W6x8.5 (W150x12.6) Steel Post, Test Nos. WAP-1 through WAP-5	46
Figure A-3. Material Specifications, 6-in. x 8-in. (152-mm x 203-mm) SYP Post, Test Nos. SYPW-1 through SYPW-4	47
Figure A-4. Material Specifications, 6-in. x 8-in. (152-mm x 203-mm) SYP Post, Test Nos. SYPW-1 through SYPW-4	48
Figure A-5. Graph of Soil Sieve Data for All Bogie Tests	49
Figure B-1. Test No. WAP-1 Results (SLICE -1)	51
Figure B-2. Test No. WAP-1 Results (SLICE -2)	52
Figure B-3. Test No. WAP-2 Results (SLICE -1)	53
Figure B-4. Test No. WAP-2 Results (SLICE -2)	54
Figure B-5. Test No. WAP-3 Results (SLICE -1)	55
Figure B-6. Test No. WAP-3 Results (SLICE -2)	56

Figure B-7. Test No. WAP-4 Results (SLICE -1)57
Figure B-8. Test No. WAP-4 Results (SLICE -2)58
Figure B-9. Test No. WAP-5 Results (SLICE -1)59
Figure B-10. Test No. WAP-5 Results (SLICE -2)60
Figure B-11. Test No. SYPW-1 Results (SLICE -2)61
Figure B-12. Test No. SYPW-2 Results (SLICE -2)62
Figure B-13. Test No. SYPW-3 Results (SLICE -2)63
Figure B-14. Test No. SYPW-4 Results (SLICE -2)64
Figure C-1. 6-in. x 8-in. (152-mm x 203-mm) SYP Post Inspection, Test No. SYP W-166
Figure C-2. 6-in. x 8-in. (152-mm x 203-mm) SYP Post Inspection, Test No. SYP W-2
through SYP W-4.....67

LIST OF TABLES

Table 1. Test Matrix.....11
Table 2. Dynamic Component Testing Results32

1 INTRODUCTION

1.1 Background

The Midwest Roadside Safety Facility (MwRSF) has utilized computer simulation during the design phases of many projects. Researchers have relied primarily on strong-axis performance of posts embedded in soil to verify post-soil reactions during an impact. As computer simulation becomes more prominently used, there is a need to refine the performance of a post embedded in soil. Thus, collecting data for the performance of a post impacted in the weak-axis is necessary.

1.2 Objective

The primary objective of this research study was to determine the soil-post impact reaction of W6x8.5 (W150x12.6) steel posts and 6-in. x 8-in. (152-mm x 203-mm) Southern Yellow Pine (SYP) posts when impacted along the weak-axis.

1.3 Scope

The primary research objective was achieved through the completion of several tasks. First, a series of bogie tests were conducted on W6x8.5 (W150x12.6) steel posts and 6-in. x 8-in. SYP posts to determine the post-soil performance along the weak-axis. An embedment depth of 40 in. (1016 mm) was selected as the starting depth since it corresponds to standard Midwest Guardrail System (MGS) post embedment. Force vs. displacement, energy vs. displacement, and failure mechanisms of the steel and SYP posts were analyzed. Finally, conclusions and recommendations were made that pertain to performance of the steel and wood posts when impacted along the weak-axis.

2 TEST CONDITIONS

2.1 Test Facility

The testing facility is located at the Lincoln Air Park on the northwest side of the Lincoln Municipal Airport, and is approximately 5 miles (8.0 km) northwest of the University of Nebraska-Lincoln.

2.2 Equipment and Instrumentation

The equipment and instrumentation utilized to collect and record data during the dynamic bogie tests included a bogie, accelerometers, a retroreflective optic speed trap, high-speed and standard-speed digital video cameras, and a still camera.

2.2.1 Bogie

A rigid-frame bogie was used to impact the posts. A variable-height detachable impact head was used in the testing. The bogie head was constructed of an 8-in. (203-mm) diameter, ½-in. (13-mm) thick standard steel pipe, with ¾-in. (19-mm) neoprene belting wrapped around the pipe to prevent local damage to the post from the impact. The impact head was bolted to the bogie, creating a rigid frame with an impact height of 24⁷/₈ in. (632 mm). The bogie with the impact head is shown in Figure 1. The weight of the bogie with the addition of the mountable impact head and accelerometers was 1,893 lb (859 kg) for tests nos. WAP-1 through WAP-5 and 1,891 lb (858 kg) for tests nos. SYPW-1 through SYPW-4.

A pickup truck with a reverse cable tow system was used to propel the bogie to a target impact speed of 20.0 mph (32.2 km/h). When the bogie approached the end of the guidance system, it was released from the tow cable, allowing it to be free-rolling when it impacted the post. A remote braking system was installed on the bogie, allowing it to be brought safely to rest after the test.



Figure 1. Rigid-Frame Bogie on Guidance Track

2.2.2 Accelerometers

One SLICE 6DX accelerometer system was mounted on the bogie vehicle near its center of gravity to measure the acceleration in the longitudinal direction for test nos. WAP-1 through WAP-5 and SYPW-1 through SYPW-4.

The SLICE 6DX is a modular data-acquisition system manufactured by Diversified Technical Systems, Inc. (DTS) of Seal Beach, California. The acceleration sensors were mounted inside the body of the custom-built SLICE 6DX event data recorder and recorded data at 10,000 Hz to the onboard microprocessor. The SLICE 6DX was configured with 7 GB of non-volatile flash memory; a range of ± 500 g's; a sample rate of 10,000 Hz; and a 1,650 Hz (CFC 1000) anti-aliasing filter. The SLICEWare computer software program and a customized Microsoft Excel worksheet were used to analyze and plot the accelerometer data.

2.2.3 Retroreflective Optic Speed Trap

The retroreflective optic speed trap was used to determine the speed of the bogie vehicle before impact. Three retroreflective targets, spaced at approximately 18-in. (457-mm) intervals, were applied to the side of the bogie. When the emitter/receiver had emitted a beam of light and received it after reflection off the vehicle targets, a signal was sent to the data acquisition

computer, recording at 10,000 Hz, and also activated the external LED box. The speed was then calculated using the spacing between the retroreflective targets and the time between the signals. LEDs and high-speed digital video analysis are only used as a backup in the event that vehicle speeds cannot be determined from the electronic data.

2.2.4 Digital Photography

One AOS VITcam high-speed digital video camera and two GoPro Hero 3 digital video cameras were used to document each test. The AOS high-speed camera had a frame rate of 500 frames per second, and the GoPro Hero 3 digital video cameras had a frame rate of 119 frames per second. Both cameras were placed laterally from the post with a view perpendicular to the bogie's direction of travel. A Nikon D50 digital still camera was also used to document pre- and post-test conditions for all tests.

2.3 End-of-Test Determination

When the impact head initially contacts the test article, the force exerted by the surrogate test vehicle is directly perpendicular. However, as the post rotates the surrogate test vehicle's orientation and path move farther from the perpendicular position. This introduces two sources of error: (1) the contact force between the impact head and the post has a vertical component, and (2) the impact head slides upward along the test article. Therefore, only the initial portion of the accelerometer trace may be used, since variations in the data become significant as the system rotates and the surrogate test vehicle overrides the system. For this reason, the end of the test needed to be defined.

Guidelines were established to define the end-of-test time using the high-speed video of the crash test. The first occurrence of any one of the following three events was used to determine the end of the test: (1) the test article fractures, (2) the surrogate vehicle overrides/loses contact with the test article, or (3) a maximum post rotation of 45 degrees occurs.

2.4 Data Processing

The electronic accelerometer data obtained in dynamic testing was filtered using the SAE Class 60 Butterworth filter conforming to the SAE J211/1 specifications [2]. The pertinent acceleration signal was extracted from the bulk of the data signals. The processed acceleration data was then multiplied by the mass of the bogie to get the impact force using Newton's Second Law. Next, the acceleration trace was integrated to find the change in velocity vs. time. The initial velocity of the bogie, calculated from the pressure tape switch data, was then used to determine the bogie velocity, and the calculated velocity trace was integrated to find the bogie's displacement. This displacement is also the displacement of the post. Combining the previous results, a force vs. deflection curve was plotted for each test. Finally, integration of the force vs. deflection curve provided the energy vs. deflection curve for each test.

Although the acceleration data was applied to the impact location, the data came from the center of gravity of the rigid bogie. Error may be potentially induced by the data since the bogie may not be perfectly rigid and sustains vibrations. The bogie may rotate during impact events, causing differences in accelerations between the bogie's center of mass and the impact head. While these issues may potentially affect the data, the effects are believed to be very small for short-duration events. Thus, the data was deemed valid for comparison purposes. Filtering procedures were applied to the electronic data to smooth out vibrations. Rotations of the bogie were minor. One useful aspect of using accelerometer data was that it included inertial influences in the post's resistive force. Mass effects were considered beneficial as they can affect barrier performance as well as influence test results.

The accelerometer data for each test was processed to obtain acceleration, velocity, and deflection curves, as well as force vs. deflection and energy vs. deflection curves.

3 COMPONENT TESTING RESULTS AND DISCUSSION

3.1 Purpose

In previous research, MwRSF has conducted numerous dynamic bogie tests of W6x8.5 (W150x12.6) steel posts and 6-in. x 8-in. (152-mm x 203-mm) SYP posts. However, no such tests had been conducted on these posts when impacted along the weak axis. Therefore, bogie tests were undertaken on W6x8.5 (W150x12.6) steel posts and 6-in. x 8-in. (152-mm x 203-mm) SYP posts impacted along the weak axis at varying embedment depths to determine their dynamic properties.

3.2 Scope

Five bogie tests were conducted on 72-in. (1,829-mm) long W6x8.5 (W150x12.6) A992 steel posts with embedment depths ranging from 24 to 40 in. (610 to 1,016 mm), as shown in Figures 2 and 3. Also, four bogie tests were conducted on 72-in. (1,829-mm) long 6-in. x 8-in. (152mm x 203mm) SYP posts embedded at depths ranging from 30 to 40 in. (762 to 1,016 mm), as shown in Figures 4 and 5. A compacted, coarse crushed limestone material, as recommended by the Manual for Assessing Safety Hardware (MASH), was utilized for all tests [1].

The target impact conditions were an impact speed of 20 mph (32.2 km/h) and an impact angle of 0 degrees, creating weak-axis bending. The posts were impacted 24⁷/₈ in. (632 mm) above the groundline and perpendicular to the web of the post. The dynamic component testing matrix and the test setup are shown in Table 1. Material specifications, mill certifications, and certificates of conformity for the posts and soil specifications are shown in Appendix A.

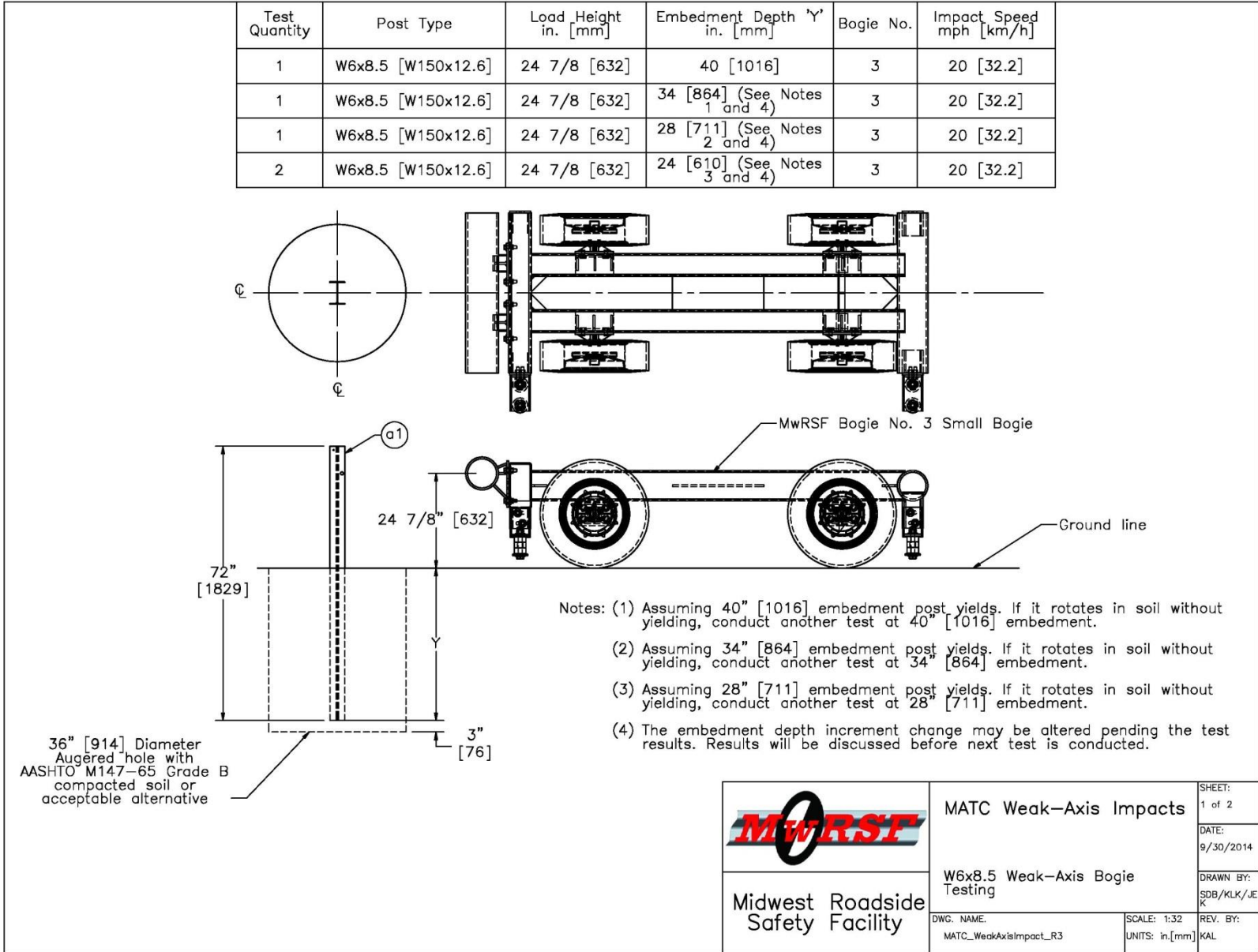


Figure 2. Bogie Test Matrix and Setup, W6x8.5 (W150x12.6) Steel Posts

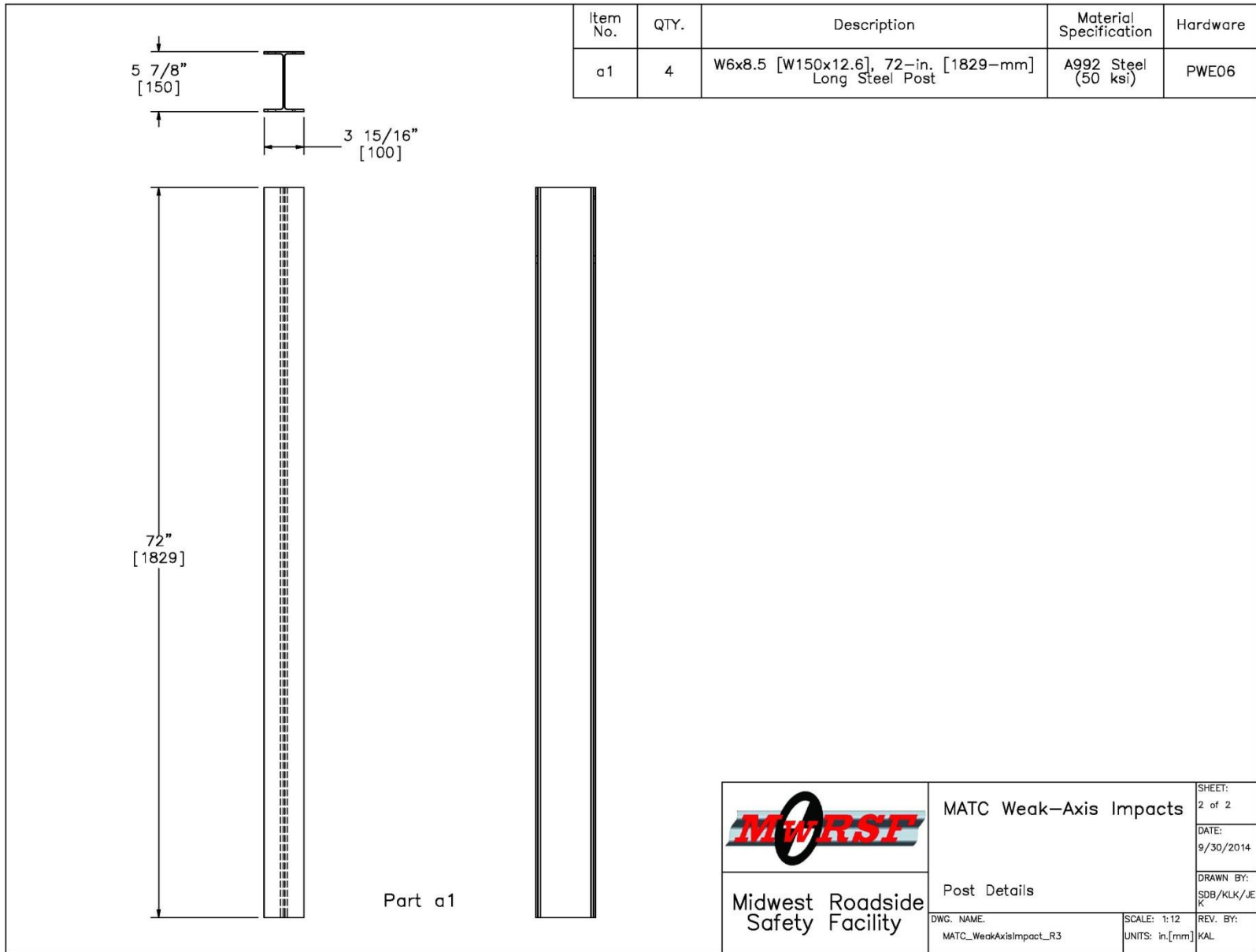


Figure 3. Weak-Axis Impact Post Details, W6x8.5 (W150x12.6) Steel Posts

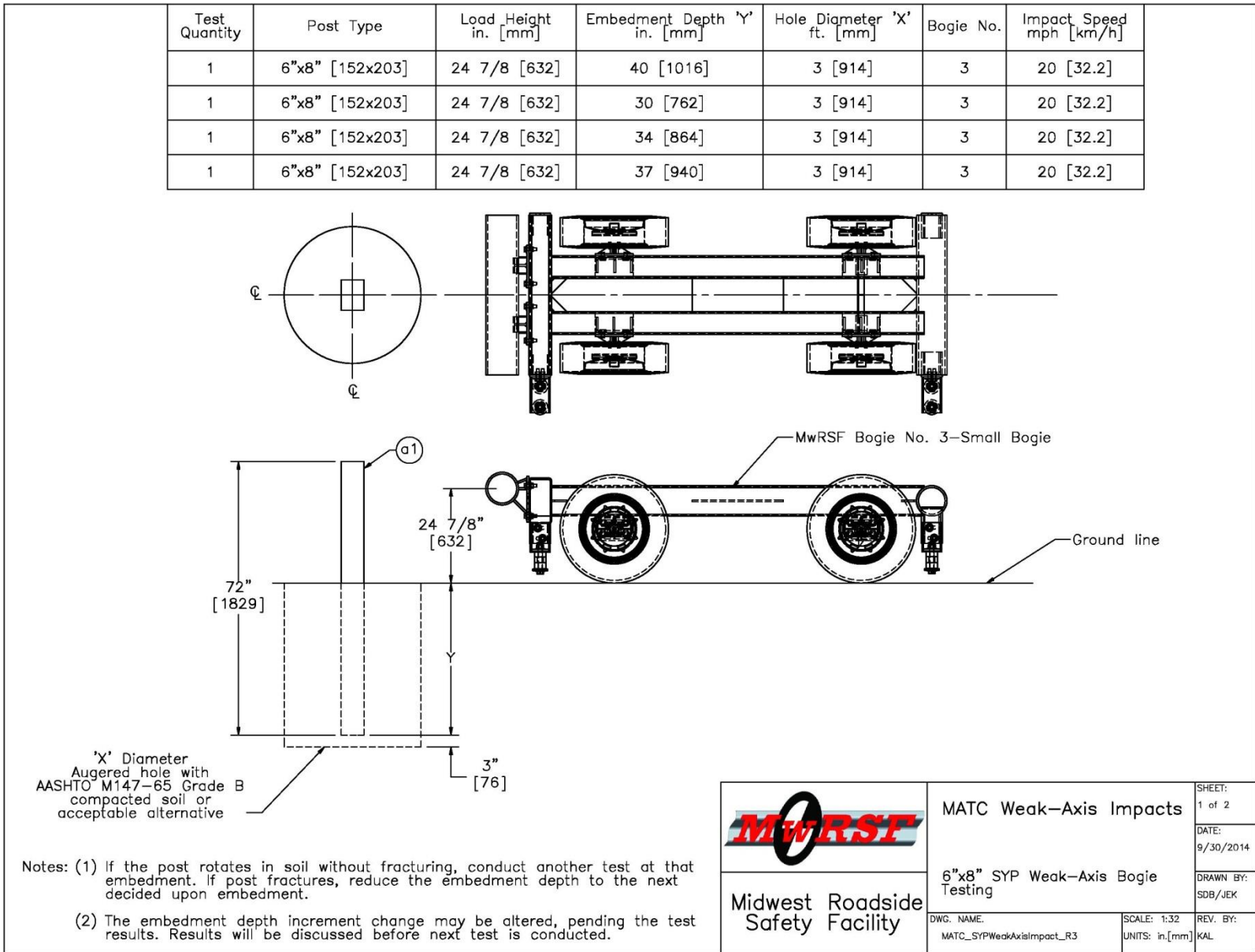


Figure 4. Bogie Test Matrix and Setup, 6-in. x 8-in. (152-mm x 203-mm) SYP Posts

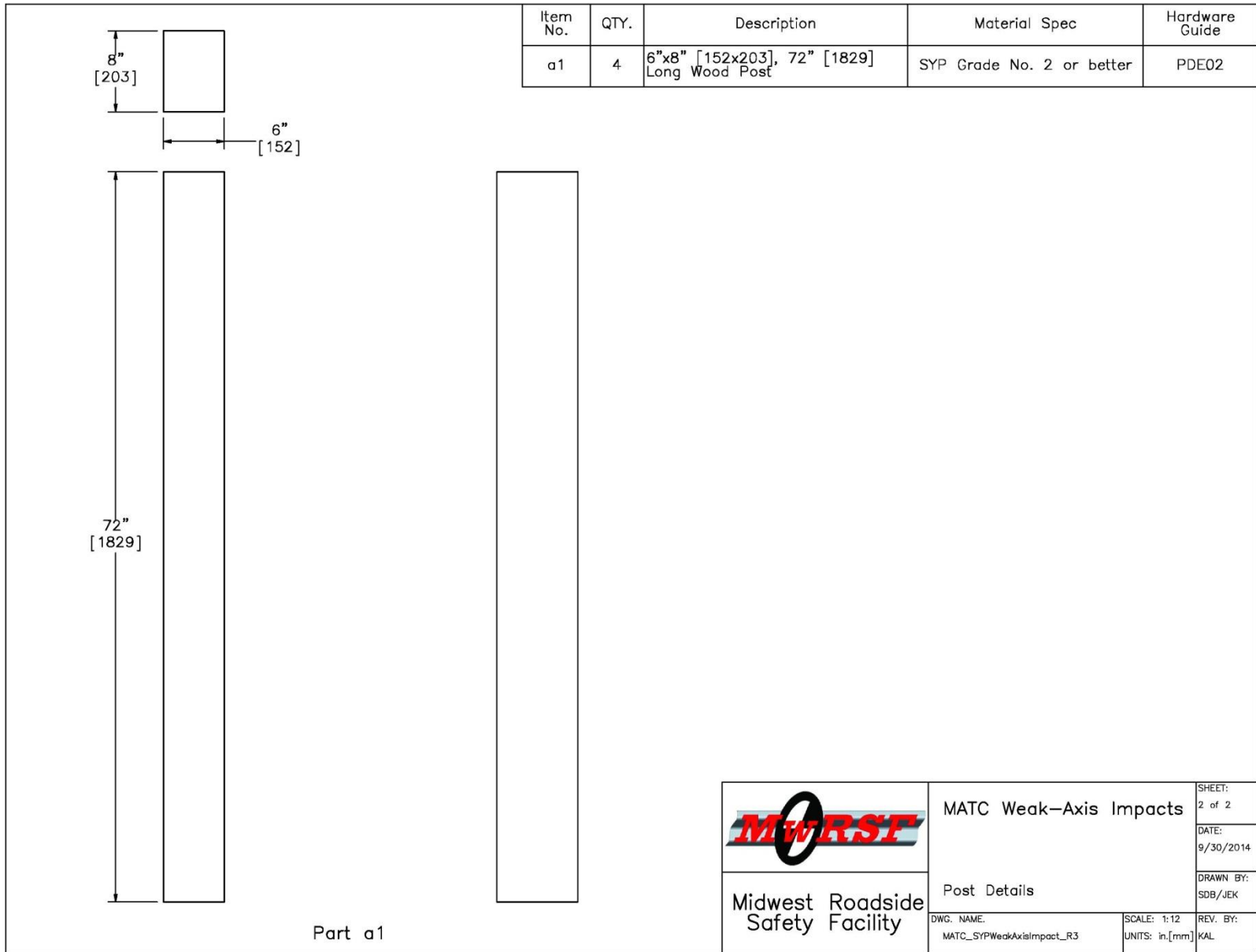


Figure 5. Weak-Axis Impact Post Details, 6-in. x 8-in. (152-mm x 203-mm). SYP Posts

Table 1. Test Matrix

Test No.	Post Material	Post Description	Post Length in. (mm)	Embedment Depth in. (mm)	Impact Orientation	Target Speed mph (km/h)	Impact Height in. (mm)
WAP-1	A992 Steel	W6x8.5 (W150x12.6)	72 (1829)	40 (1016)	Weak Axis	20 (32.2)	24 ⁷ / ₈ (632)
WAP-2	A992 Steel	W6x8.5 (W150x12.6)	72 (1829)	34 (864)	Weak Axis	20 (32.2)	24 ⁷ / ₈ (632)
WAP-3	A992 Steel	W6x8.5 (W150x12.6)	72 (1829)	28 (711)	Weak Axis	20 (32.2)	24 ⁷ / ₈ (632)
WAP-4	A992 Steel	W6x8.5 (W150x12.6)	72 (1829)	24 (610)	Weak Axis	20 (32.2)	24 ⁷ / ₈ (632)
WAP-5	A992 Steel	W6x8.5 (W150x12.6)	72 (1829)	24 (610)	Weak Axis	20 (32.2)	24 ⁷ / ₈ (632)
SYPW-1	Southern Yellow Pine Wood	6-in. x 8-in. (152mm x 203mm)	72 (1829)	40 (1016)	Weak Axis	20 (32.2)	24 ⁷ / ₈ (632)
SYPW-2	Southern Yellow Pine Wood	6-in. x 8-in. (152 mm x 203 mm)	72 (1829)	30 (762)	Weak Axis	20 (32.2)	24 ⁷ / ₈ (632)
SYPW-3	Southern Yellow Pine Wood	6-in. x 8-in. (152 mm x 203 mm)	72 (1829)	34 (864)	Weak Axis	20 (32.2)	24 ⁷ / ₈ (632)
SYPW-4	Southern Yellow Pine Wood	6-in. x 8-in. (152 mm x 203 mm)	72 (1829)	37 (940)	Weak Axis	20 (32.2)	24 ⁷ / ₈ (632)

3.3 Results

Results from all nine dynamic component tests are discussed in the following subsections. The force and displacement data shown in this section was calculated from the SLICE accelerometer unit. Results for all accelerometers used on each test are provided in Appendix B.

3.3.1 Test No. WAP-1

During test no. WAP-1, the bogie impacted the W6x8.5 (W150x12.6) steel post embedded 40 in. (1,016 mm) at a speed of 20.4 mph (32.8 km/h). Upon impact, the post began to rotate through the soil. Post rotation continued until the bogie overrode the post at a displacement of 36.5 in. (927 mm). The post bent and yielded approximately 8 in. (203 mm) below the groundline.

Force vs. deflection and energy vs. deflection curves created from the SLICE accelerometer data are shown in Figure 6. The forces rose to a peak force of 5.8 kips (25.8 kN) at 2.0 in. (51 mm) of deflection. The average resistive force decreased to approximately 4 kips (17.8kN). A total of 110.1 kip-in. (12.4 kJ) of energy was absorbed by the system before the bogie overrode the post at 36.5 in. (927 mm). Time-sequential and post-impact photographs are shown in Figure 7.

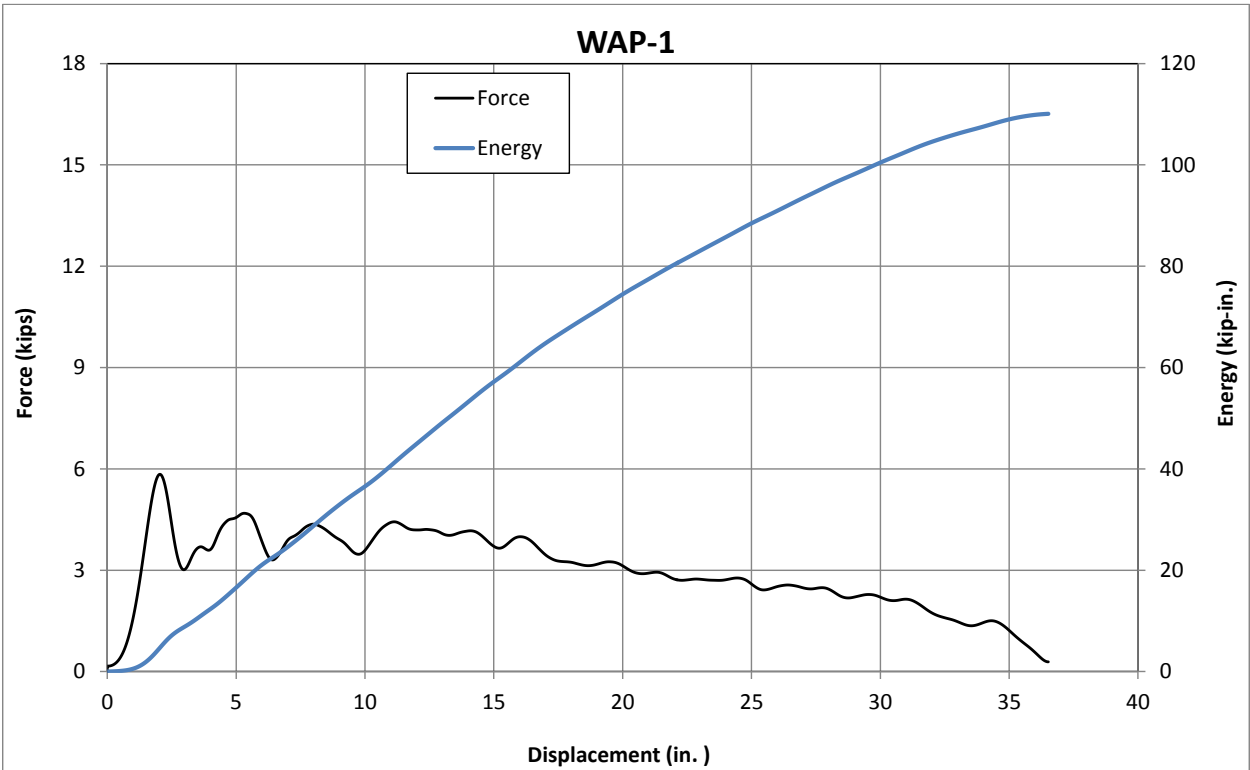
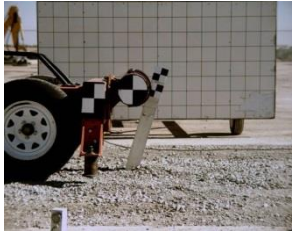


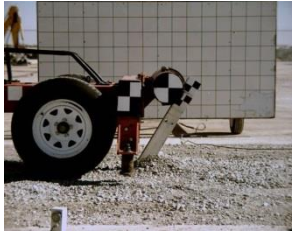
Figure 6. Force vs. Deflection and Energy vs. Deflection, Test No. WAP-1



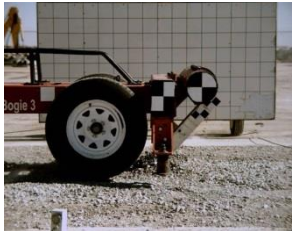
IMPACT



0.030 sec



0.060 sec



0.090 sec



0.120 sec



0.150 sec



Figure 7. Time-Sequential and Post-Impact Photographs, Test No. WAP-1

3.3.2 Test No. WAP-2

During test no. WAP-2, the bogie impacted the W6x8.5 (W150x12.6) steel post embedded 34 in. (864 mm) at a speed of 20.2 mph (32.5 km/h). Post rotation continued until the bogie overrode the post at a displacement of 41.5 in. (1,054 mm). The post bent and yielded approximately 8 in. (203 mm) below the groundline.

Force vs. deflection and energy vs. deflection curves created from the SLICE accelerometer data are shown in Figure 8. The forces rose to a peak force of 9.7 kips (43.1 kN) at 1.7 in. (43 mm) of deflection. The posts provided an average resistive force of around 4.0 kips (17.8 kN) through 12.0 in. (305 mm) of deflection. A total of 113.1 kip-in. (12.8 kJ) of energy was absorbed by the system before the bogie overrode the post at 41.5 in. (1,054 mm). Time-sequential and post-impact photographs are shown in Figure 9.

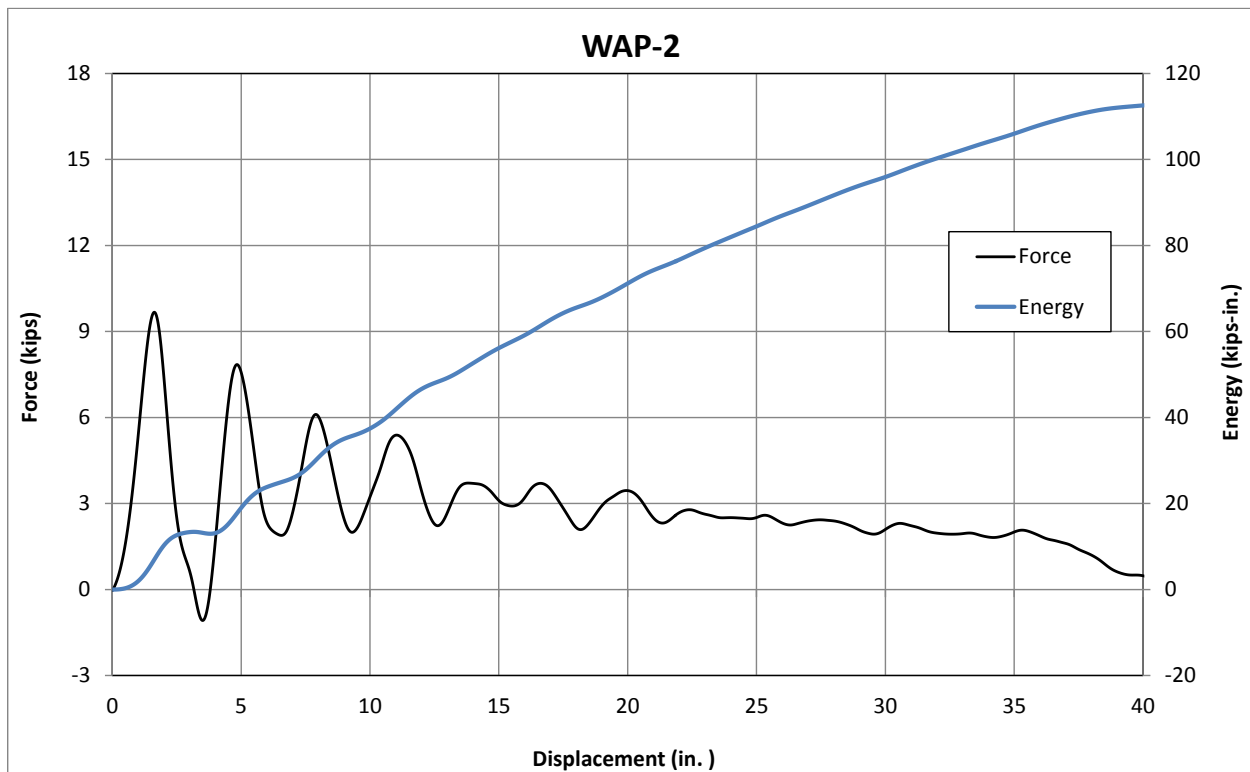


Figure 8. Force vs. Deflection and Energy vs. Deflection, Test No. WAP-2



IMPACT



0.030 sec



0.060 sec



0.090 sec



0.120 sec



0.150 sec



Figure 9. Time-Sequential and Post-Impact Photographs, Test No. WAP-2

3.3.3 Test No. WAP-3

During test no. WAP-3, the bogie impacted the W6x8.5 (W150x12.6) steel post embedded 28 in. (711 mm) at a speed of 20.6 mph (33.2 km/h). Upon impact, the post began to rotate through the soil. Post rotation continued until the bogie overrode the top of the post at a displacement of 41.5 in. (1,054 mm). The post bent slightly and encountered minor yielding below the groundline.

Force vs. deflection and energy vs. deflection curves created from the SLICE accelerometer data are shown in Figure 10. The forces rose to a peak force of 12.2 kips (54.3 kN) at 1.7 in. (43 mm) of deflection. The post provided an average resistive force of 4.0 kips (17.8kN) through 12.0 in. (305 mm) of deflection. The force then steadily decreased for the remainder of the impact event. A total of 103.1 kip-in. (11.6 kJ) of energy was absorbed before the bogie overrode the post at 41.5 in. (1,054 mm). Time-sequential and post-impact photographs are shown in Figure 11.

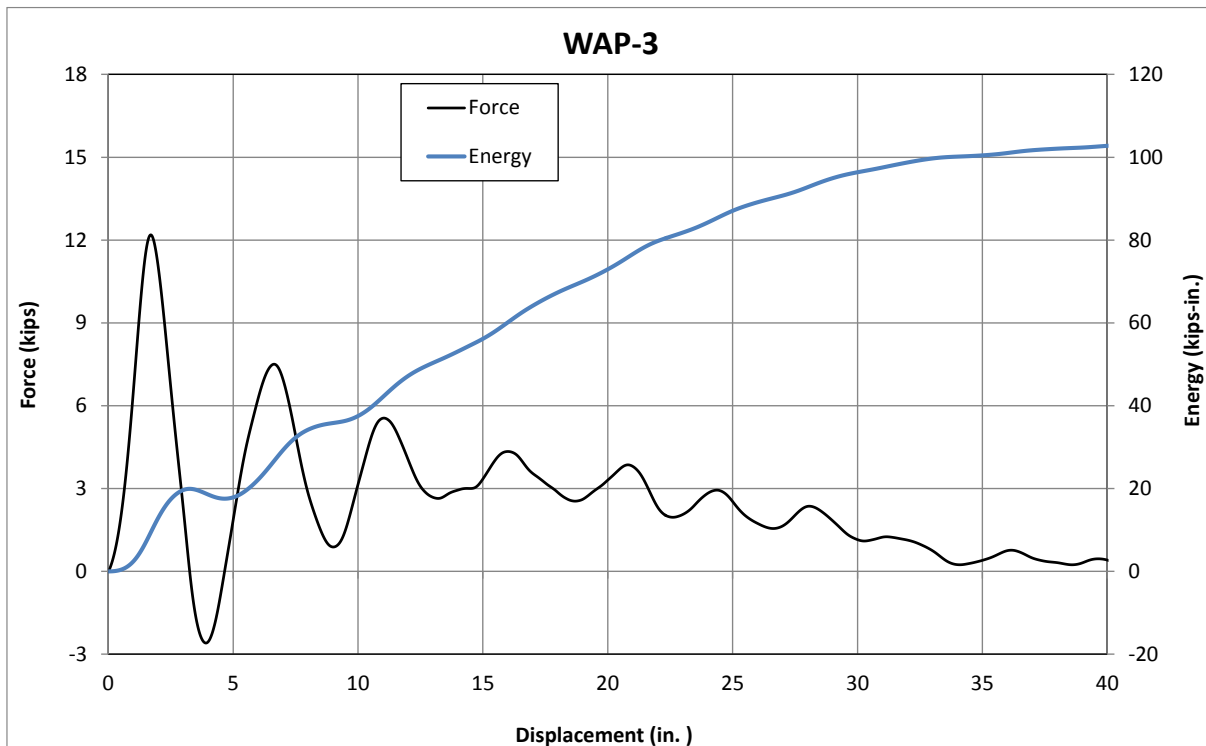


Figure 10. Force vs. Deflection and Energy vs. Deflection, Test No. WAP-3



IMPACT



0.030 sec



0.060 sec



0.090 sec



0.120 sec



0.150 sec



Figure 11. Time-Sequential and Post-Impact Photographs, Test No. WAP-3

3.3.4 Test No. WAP-4

During test no. WAP-4, the bogie impacted the W6x8.5 (W150x12.6) steel post embedded 24 in. (610 mm) at a speed of 20.5 mph (33.0 km/h). Upon impact, the post began to rotate through the soil. The post continued to rotate until the bogie overrode the post at a displacement of 41.2 in. (1,046 mm). The post bent slightly and encountered minor yielding below the groundline.

Force vs. deflection and energy vs. deflection curves created from the SLICE accelerometer data are shown in Figure 12. The forces rose to a peak force of 15.4 kips (68.5 kN) at 1.8 in. (46 mm) of deflection. The post provided an average force of approximately 3.8 kips (16.9 kN) through 27 in. (686 mm) of deflection. The force then steadily decreased for the remainder of the impact event. A total of 95.1 kip-in. (10.7 kJ) of energy was absorbed by the system before the bogie overrode the post at 41.2 in. (1,046 mm). Time-sequential and post-impact photographs are shown in Figure 13.

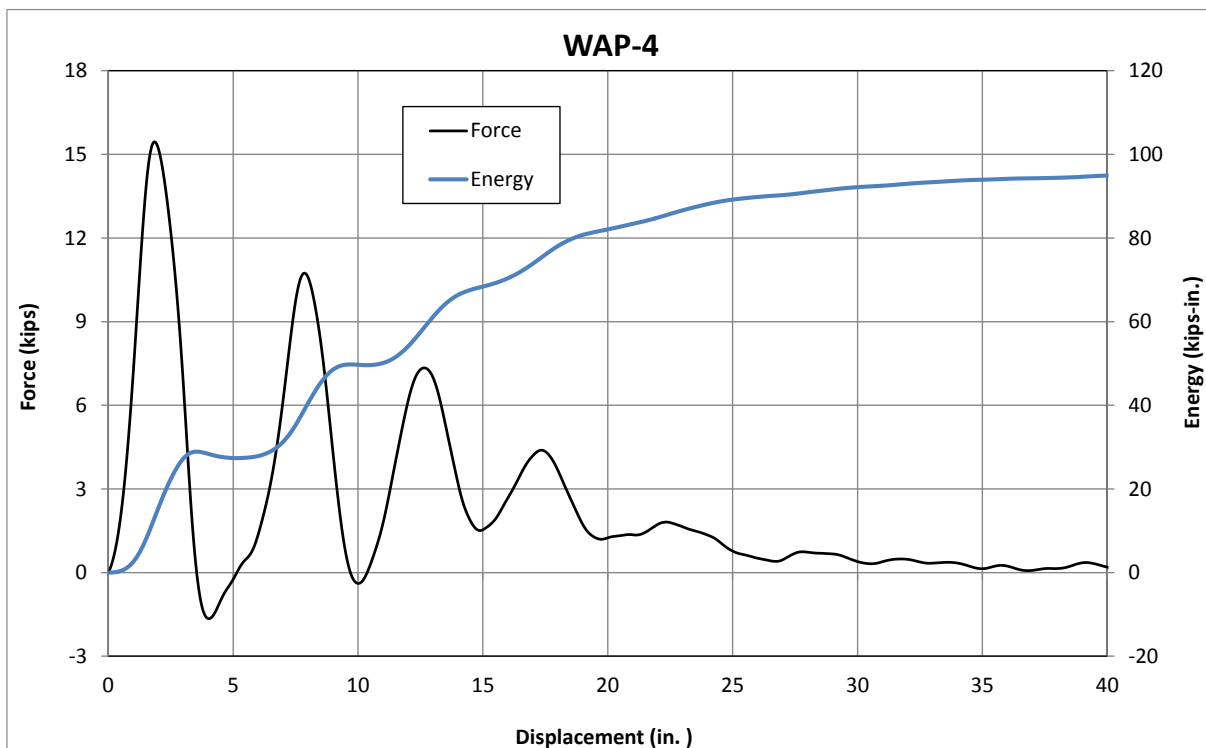
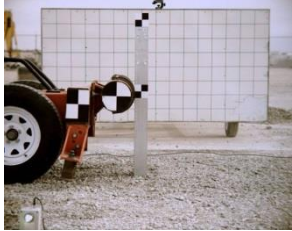


Figure 12. Force vs. Deflection and Energy vs. Deflection, Test No. WAP-4



IMPACT



0.030 sec



0.060 sec



0.090 sec



0.120 sec



0.150 sec



Figure 13. Time-Sequential and Post-Impact Photographs, Test No. WAP-4

3.3.5 Test No. WAP-5

During test no. WAP-5, the bogie impacted the W6x8.5 (W150x12.6) steel post embedded 24 in. (610 mm) at a speed of 20.3 mph (32.7 km/h). Upon impact, the post began to rotate through the soil. The post continued to rotate until the bogie overrode the post at a displacement of 37.7 in. (958 mm). The post bent backwards slightly and encountered minor yielding below the groundline.

Force vs. deflection and energy vs. deflection curves created from the accelerometer data are shown in Figure 14. The force rose to a peak force of 15.4 kips (68.5 kN) at 1.7 in. (43 mm) of deflection. The post provided an average resistive force of 4.4 kips (19.6 kN) through 16 in. (406 mm) of deflection. The force then steadily decreased for the remainder of the impact event. A total of 87.7 kip-in. (9.9 kJ) of energy was absorbed by the system before the bogie overrode the post at 37.7 in (958 mm). Time-sequential and post-impact photographs are shown in Figure 15.

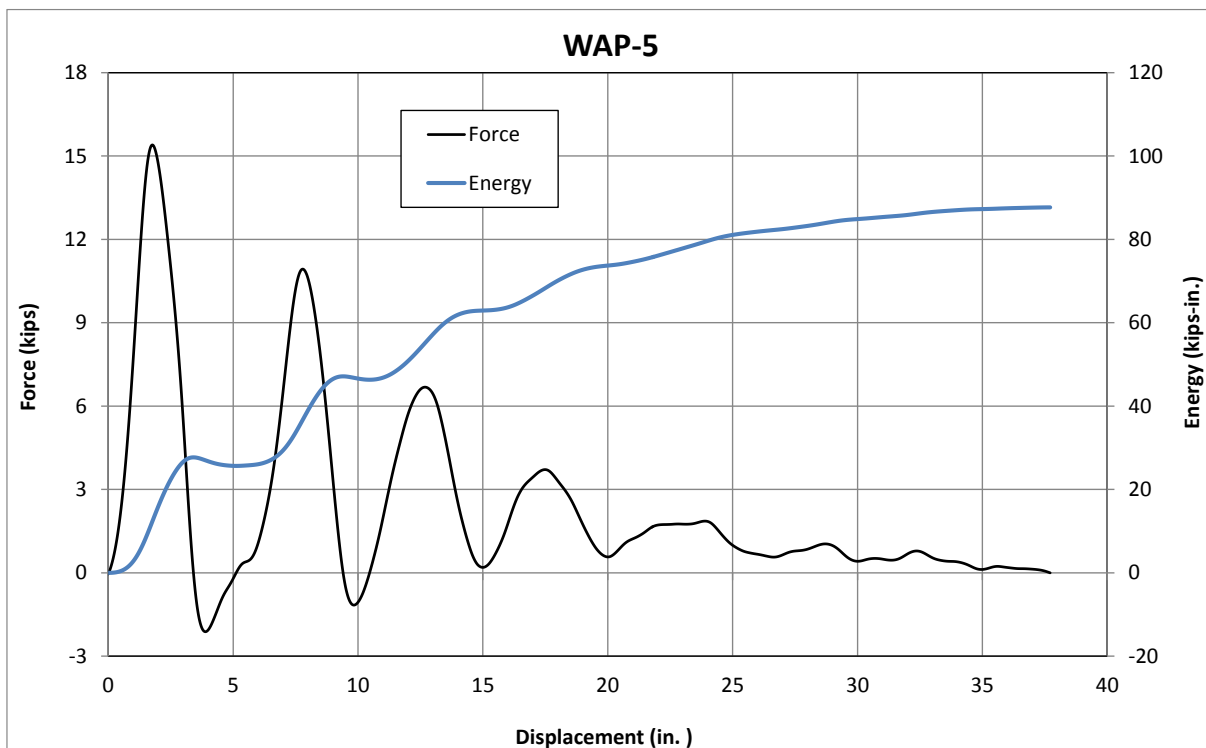


Figure 14. Force vs. Deflection and Energy vs. Deflection, Test No. WAP-5



IMPACT



0.030 sec



0.060 sec



0.090 sec



0.120 sec



0.150 sec



Figure 15. Time-Sequential and Post-Impact Photographs, Test No. WAP-5

3.3.1 Test No. SYPW-1

During test no. SYPW-1, the bogie impacted the 6-in. x 8-in. (152-mm x 203-mm) SYP post embedded 40 in. (1016 mm) at a speed of 20.5 mph (33.0 km/h). Upon impact, the post began to rotate through the soil. The post continued to rotate until it fractured at a displacement of 10.5 in. (267 mm). The post fractured approximately 6 in. (152 mm) below the groundline.

Force vs. deflection and energy vs. deflection curves created from the SLICE accelerometer data and are shown in Figure 16. A peak force of 14.3 kips (63.6 kN) was observed at 4.2 in. (107 mm) of deflection. At this point, the post began to fracture, and the resistive forces declined. The post continued to provide resistance until fracture was completed at a deflection of 10.5 in. (267 mm). A total of 82.1 kip-in. (9.3 kJ) of energy was absorbed by the post and soil by the conclusion of post fracture. Time-sequential and post-impact photographs are shown in Figure 17.

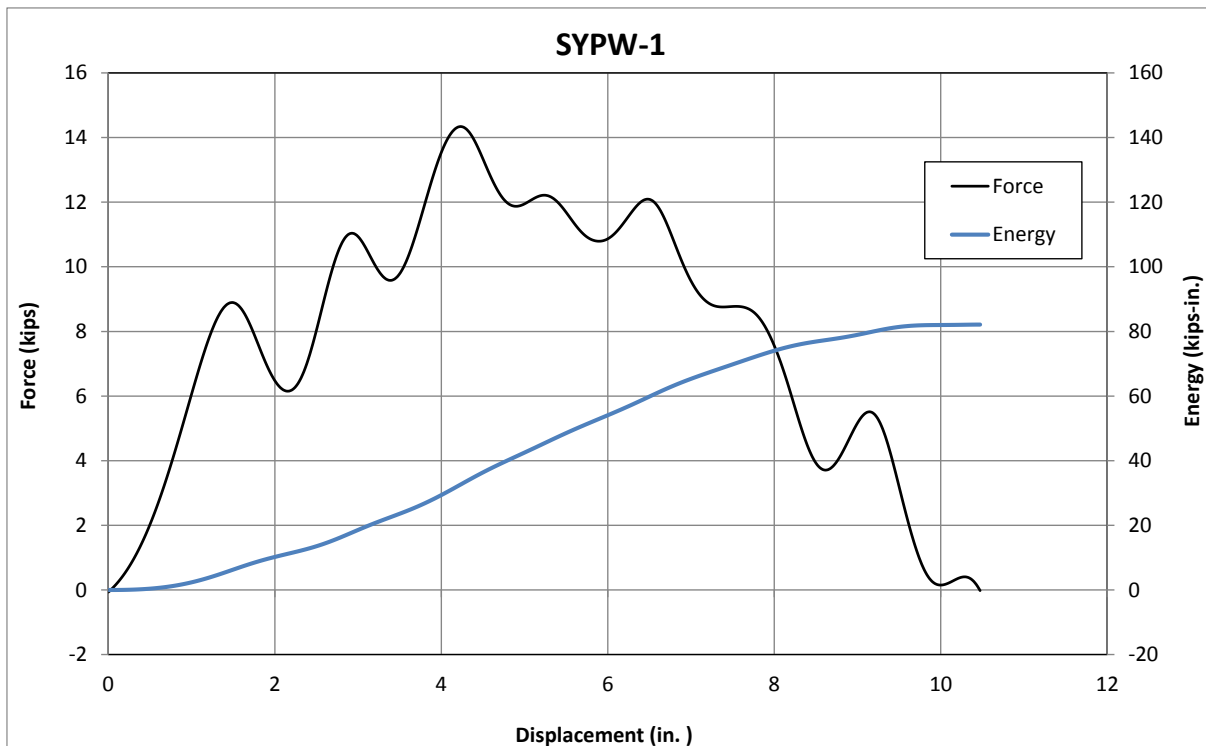
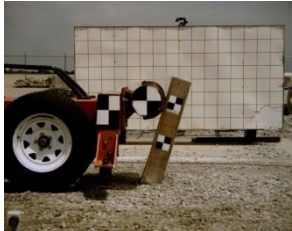


Figure 16. Force vs. Deflection and Energy vs. Deflection, Test No. SYPW-1



IMPACT



0.030 sec



0.060 sec



0.090 sec



0.120 sec



0.150 sec



Figure 17. Time-Sequential and Post-Impact Photographs, Test No. SYPW-1

3.3.2 Test No. SYPW-2

During test no. SYPW-2, the bogie impacted the 6-in. x 8-in. (152-mm x 203-mm) SYP post embedded 30 in. (762 mm) at a speed of 20.8 mph (33.5 km/h). Upon impact, the post began to rotate through the soil. The post continued to rotate until it fractured at a displacement of 36.6 in. (930 mm). The SYP post showed no signs of fracture.

Force vs. deflection and energy vs. deflection curves created from the SLICE accelerometer data are shown in Figure 18. Initially, the resistive force increased and reached a peak force of 15.7 kips (69.8 kN) at 1.0 in. (25 mm) of deflection. After this peak, the resistive force steadily decreased for the remainder of the impact event. A total of 121 kip-in. (13.7 kJ) of energy was absorbed by the system before the bogie overrode the post at 36.6 in. (930 mm). Time-sequential and post-impact photographs are shown in Figure 19.

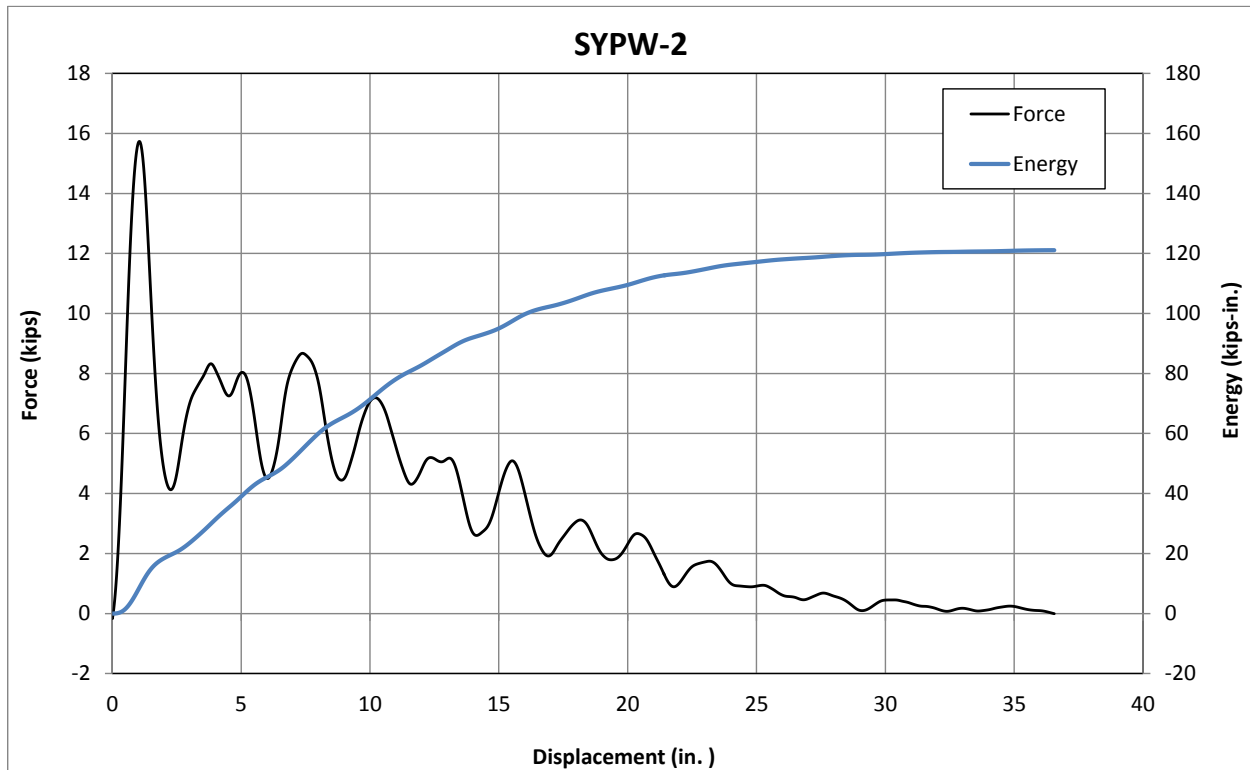


Figure 18. Force vs. Deflection and Energy vs. Deflection, Test No. SYPW-2



IMPACT



0.030 sec



0.060 sec



0.090 sec



0.120 sec



0.150 sec



Figure 19. Time-Sequential and Post-Impact Photographs, Test No. SYPW-2

3.3.3 Test No. SYPW-3

During test no. SYPW-3, the bogie impacted the 6-in. x 8-in. (152-mm x 203-mm) SYP post embedded 34 in. (864 mm) at a speed of 20.0 mph (32.2 km/h). Upon impact, the post began to rotate through the soil. Post rotation continued until the bogie overrode the post at a displacement of 40.3 in. (1,024 mm). The SYP post showed no signs of fracture.

Force vs. deflection and energy vs. deflection curves created from the SLICE accelerometer data are shown in Figure 20. Initially, the resistive force increased and reached a peak force of 15.9 kips (70.7 kN) at 1.5 in. (38 mm) of deflection. After this peak, the post provided an average resistive force of approximately 7.6 kips (33.8 kN) through 13 in. (330 mm) of deflection. The force then steadily decreased for the remainder of the impact event. A total of 162.5 kip-in. (18.4 kJ) of energy was absorbed by the system before the bogie overrode the post at 40.3 in. (1024 mm). Time-sequential and post-impact photographs are shown in Figure 21.

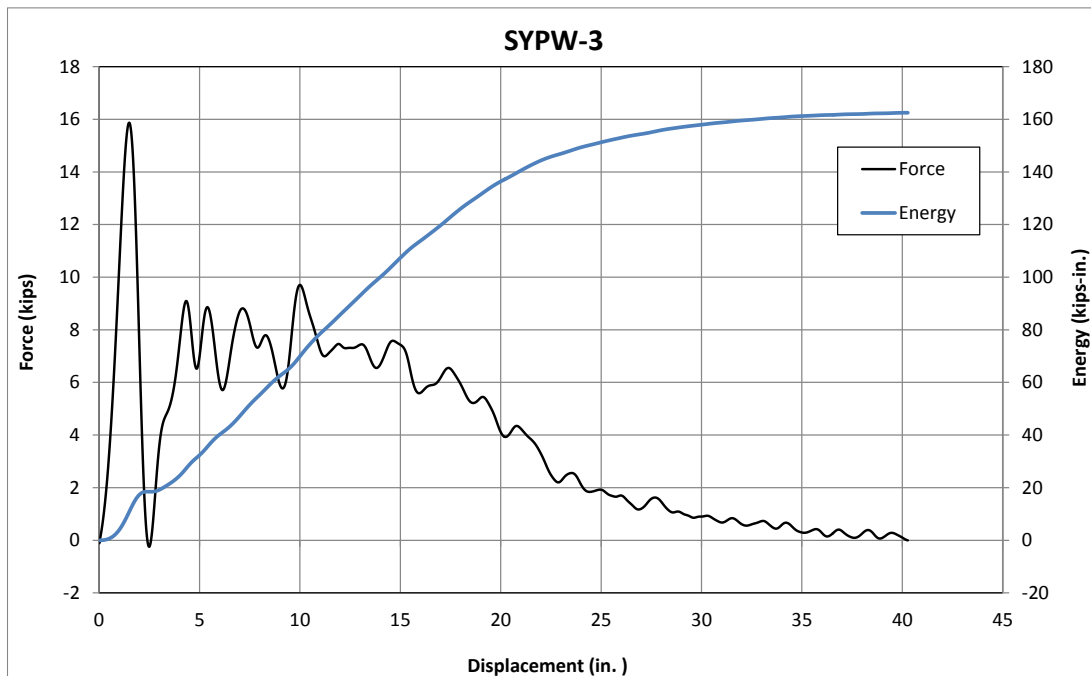


Figure 20. Force vs. Deflection and Energy vs. Deflection, Test No. SYPW-3



IMPACT



0.030 sec



0.060 sec



0.090 sec



0.120 sec



0.150 sec



Figure 21. Time-Sequential and Post-Impact Photographs, Test No. SYPW-3

3.3.4 Test No. SYPW-4

During test no. SYPW-4, the bogie impacted the 6-in. x 8-in (152-mm x 203-mm) SYP post embedded 37 in. (940 mm) at a speed of 20.3 mph (32.7 km/h). Upon impact, the post began to rotate through the soil. The post continued to rotate until it fractured at a displacement of 6.9 in. (175 mm). The post fractured approximately 8 in. (203 mm) below the groundline.

Force vs. deflection and energy vs. deflection curves created from the SLICE accelerometer data are shown in Figure 22. Initially, the resistive force increased and reached a peak force of 12.5 kips (55.6 kN) at 1.6 in. (41 mm) of deflection. Two additional peaks of approximately 12 kips (53.4 kN) occurred through 4.6 in. (117 mm) of deflection. At this point, the post began to fracture and resistive forces declined. The post continued to provide resistance until fracture was completed at a deflection of 6.9 in. (175 mm). A total of 45.4 kip-in. (5.1 kJ) of energy was absorbed by the system by the conclusion of the post fracture. Time-sequential and post-impact photographs are shown in Figure 23.

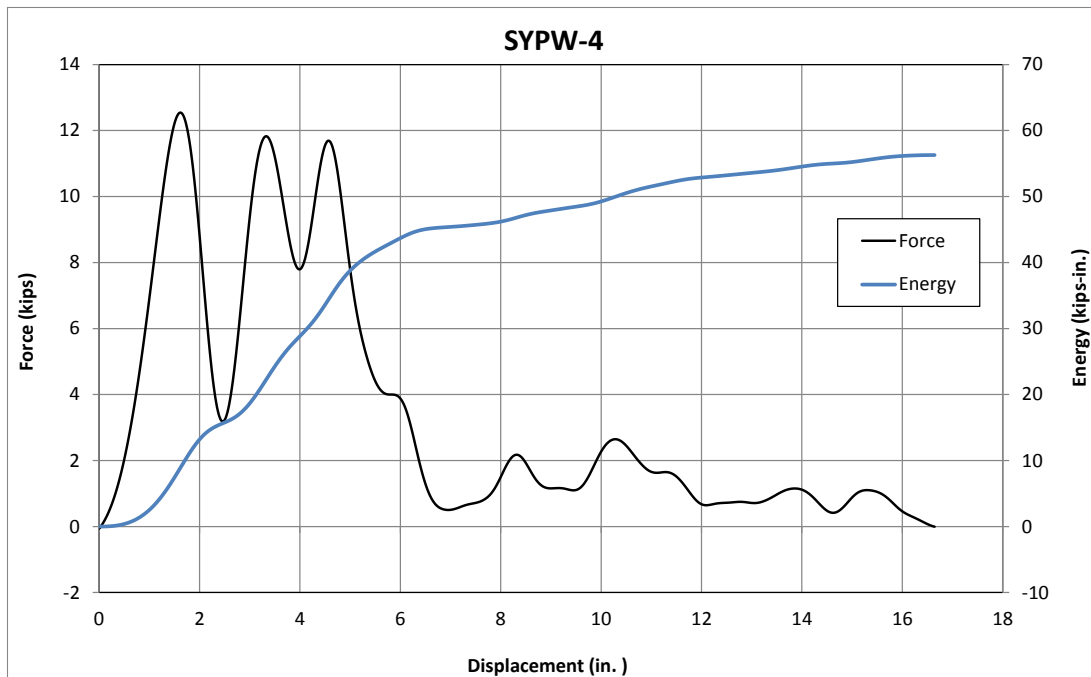


Figure 22. Force vs. Deflection and Energy vs. Deflection, Test No. SYPW-4



IMPACT



0.030 sec



0.060 sec



0.090 sec



0.120 sec



0.150 sec



Figure 23. Time-Sequential and Post-Impact Photographs, Test No. SYPW-4

3.4 Discussion

3.4.1 Steel Posts (Test Nos. WAP-1 through WAP-5)

Five tests were conducted on W6x8.5 (W150x12.6) steel posts with different embedment depths ranging between 24 and 40 in. (610 and 1,016 mm). All five posts were impacted perpendicular to the web of the post, creating weak-axis bending in order to determine the weak-axis characteristics of the steel post. All five posts rotated through the soil. However, the posts in test nos. WAP-1 and WAP-2 yielded significantly. The results are summarized in Table 2. Force vs. deflection and energy vs. deflection curves are shown in Figures 24 and 25, respectively.

It is important to understand the process and factors that reduce the bogie's kinetic energy. The energy in the system begins in the form of kinetic energy from the bogie moving in relation to the post system. When the bogie impacts the post, the bogie's kinetic energy is converted into other forms of energy. The two most prominent being the energy transferred from the bogie to the soil when the post rotates through the soil, and the energy absorbed through plastic deformation of the post. Other less prominent energies include friction between the bogie and the post and rolling friction. The system behavior resulted in varying amounts of energies absorbed by the system with total absorbed energies ranging between 113.1 kip-in. and 87.7 kip-in. (12.8 and 9.8 kJ).

System behavior is determined by the post behavior, which is dependent on post embedment depth. When the embedment depth was 40 and 34 in. (1016 and 864 mm), as used in test nos. WAP-1 and WAP-2, the posts had relatively low rotation in the soil and bent backward near the groundline. As a result of the similar behavior, the two systems absorbed approximately the same amount of total energy with values of 110.1 and 113.1 kip-in. (12.4 and 12.8 kJ), respectively. The majority of the energy was converted from kinetic energy into plastic energy from the post bending backward because the post had relatively very little rotation in the soil.

When embedment depths of 24 and 28 in. (610 and 711 mm) were used, as observed in test nos. WAP-3 through WAP-5, the posts rotated through the soil with minor post bending. The shallower embedded posts, which rotated through the soil, absorbed noticeably less energy than the posts that bent with plastic deformation, as reported in Table 2.

The resistive force reached its maximum amplitude between the first 1.7 and 2.0 in. (43 and 51 mm) of deflection, as shown in Figure 24. Generally, the amplitude of the initial peak is inversely proportional to the embedment depth. This could be attributed to the inertial effects of the bogie impacting the post. As the embedment depth decreases, additional mass is located above the bogie impact location. This additional mass above the impact point may increase the inertia required to initially displace the post, causing a higher initial resistive force. However, the deeper embedded posts provided greater resistive forces throughout the later stages of the impact event.

Table 2. Dynamic Component Testing Results

Test No.	Post Description	Embedment Depth in. (mm)	Failure Type	Peak Force kips (kN)	Average Force kip (kN)				Energy kips-in. (kJ)					Maximum Deflection in. (mm)
					@ 5"	@ 10"	@ 15"	@ 20"	@ 5"	@ 10"	@ 15"	@ 20"	Total	
WAP-1	W6x8.5 (W150x12.6)	40 (1016)	Post yielding - Flange tearing	5.8 (25.8)	3.32 (14.8)	3.65 (16.2)	3.81 (16.9)	3.72 (16.5)	16.6 (1.9)	36.5 (4.1)	57.1 (6.5)	74.4 (8.4)	110.1 (12.4)	36.5 (927)
WAP-2	W6x8.5 (W150x12.6)	34 (864)	Post yielding - Flange tearing	9.7 (43.1)	3.79 (16.9)	3.74 (16.6)	3.74 (16.6)	3.55 (15.8)	18 (2.0)	37.4 (4.2)	56.1 (6.3)	71.1 (8.0)	113.1 (12.8)	41.5 (1054)
WAP-3	W6x8.5 (W150x12.6)	28 (711)	Rotation in Soil - Minor yielding	12.2 (54.3)	3.57 (15.9)	3.75 (16.7)	3.74 (16.6)	3.64 (16.2)	17.8 (2.0)	37.5 (4.2)	56.2 (6.3)	72.9 (8.2)	103.1 (11.6)	41.5 (1054)
WAP-4	W6x8.5 (W150x12.6)	24 (610)	Rotation in Soil - Minor yielding	15.4 (68.5)	5.48 (24.4)	4.97 (22.1)	4.56 (20.3)	4.1 (18.2)	27.4 (3.1)	49.7 (5.6)	68.4 (7.7)	82.1 (9.3)	95.1 (10.7)	41.2 (1046)
WAP-5	W6x8.5 (W150x12.6)	24 (610)	Rotation in Soil - Slight yielding	15.4 (68.5)	5.13 (22.8)	4.66 (20.7)	4.19 (18.6)	3.69 (16.4)	25.7 (2.9)	46.6 (5.3)	62.9 (7.1)	73.7 (8.3)	87.7 (9.9)	41.0 (1041)
SYPW-1	6-in. x 8-in. (152mm x 203mm)	40 (1016)	Post fracture near groundline	14.3 (63.6)	8.5 (37.8)	8.2 (36.5)	NA	NA	42.5 (4.8)	82 (9.3)	NA	NA	82.1 (9.3)	10.5 (267)
SYPW-2	6-in. x 8-in. (152 mm x 203 mm)	30 (762)	Post rotation through soil	15.7 (69.8)	7.79 (34.7)	7.13 (31.7)	6.33 (28.2)	5.48 (24.4)	39 (4.4)	71.3 (8.1)	94.9 (10.7)	109.5 (12.4)	121.1 (13.7)	36.6 (930)
SYPW-3	6-in. x 8-in. (152 mm x 203 mm)	34 (864)	Post rotation through soil	15.9 (70.7)	6.47 (28.8)	6.99 (31.1)	7.15 (31.8)	6.82 (30.3)	32.3 (3.6)	69.9 (7.9)	107.2 (12.1)	136.3 (15.4)	162.5 (18.4)	40.3 (1024)
SYPW-4	6-in. x 8-in. (152 mm x 203 mm)	37 (940)	Post fracture below groundline	12.5 (55.6)	7.74 (34.4)	NA	NA	NA	38.7 (4.4)	NA	NA	NA	45.4 (5.1)	6.9 (175)

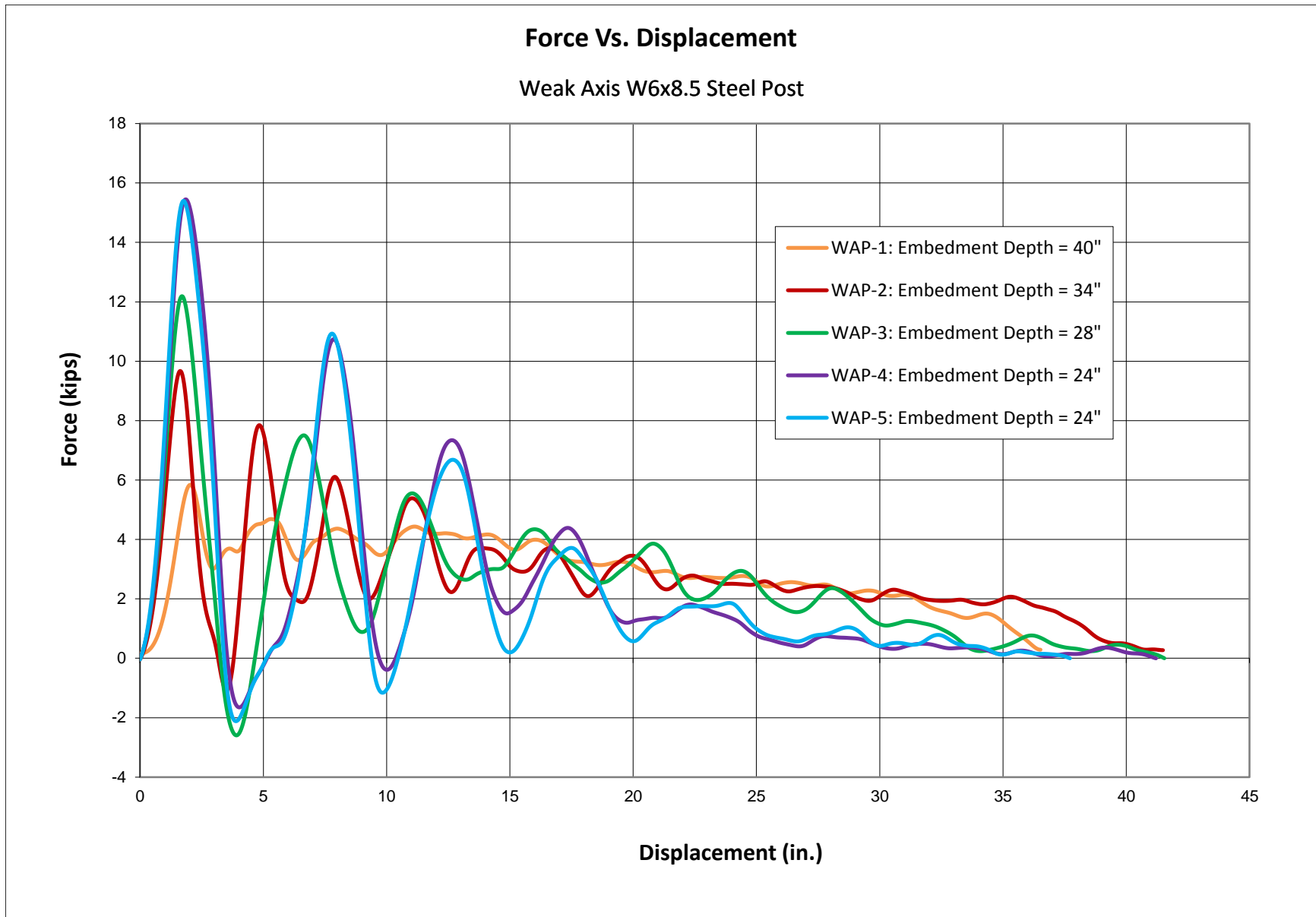


Figure 24. Force vs. Deflection Comparison, WAP-1 through WAP-5

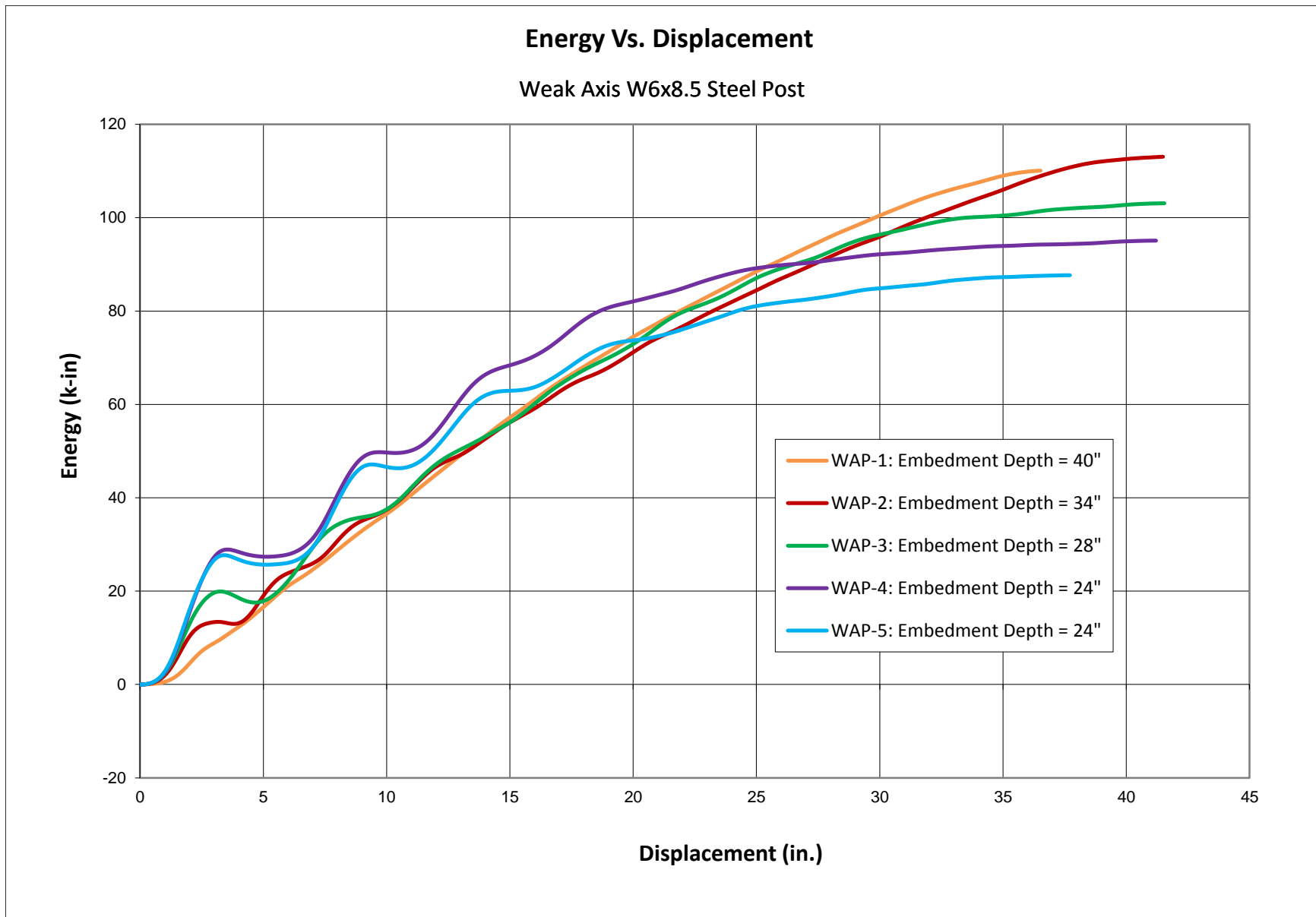


Figure 25. Energy vs. Deflection Comparison, Test Nos. WAP-1 through WAP-5

3.4.2 Wood Posts (SYPW-1 through SYPW-4)

Four tests were conducted on 6-in. x 8-in. (152-mm x 203-mm) SYP post with different embedment depths ranging between 30 and 40 in. (762 and 1,016 mm). All four posts were impacted perpendicular to the weak axis of the post, creating weak-axis bending in order to determine the weak-axis characteristics of the wood post. All four posts rotated through the soil. However, the posts in test nos. SYPW-1 and SYPW-4 fractured completely, as shown in Figure 26. The results are summarized in Table 2. Force vs. deflection and energy vs. deflection curves are shown in Figures 27 and 28, respectively.

It is important to understand the process and factors that reduce the bogie's kinetic energy. The energy in the system begins in the form of kinetic energy from the bogie moving in relation to the post system. When the bogie impacts the post, the bogie's kinetic energy is converted into other forms of energy. The two most prominent being the energy transferred from the bogie to the soil when the post rotates through the soil and the energy absorbed by the wood post bending and fracturing. Other less prominent energies include friction between the bogie and the post and rolling friction. The system behavior resulted in varying amounts of energies absorbed by the system with total absorbed energies ranging between 45.4 kip-in. and 162.5 kip-in. (5.1 and 18.4 kJ).

System behavior is determined by post behavior, which is dependent on post embedment depth. When the embedment depth was 30 and 34 in. (762 and 864 mm), as used in test nos. SYPW-2 and SYPW-3, the post experienced large rotations through the soil. The 34 in. (864 mm) embedded post allowed more energy absorption than the 30 in. (762 mm) embedded post because the deeper post displaced an additional 4 in. (102 mm) of soil compared to the shallower post during rotation. This additional soil provided greater resistive forces while the post rotated

through the soil. The total energy absorbed by the 34-in. and 30-in. (864-mm and 762-mm) embedment systems were 162.0 kip-in and 121.1 kip-in (18.4 kJ and 13.7 kJ), respectively.

When deeper embedment depths of 37 and 40 in. (940 and 1016 mm) were used, such as in test nos. SYPW-1 and SYPW-4, the post fractured completely with little rotation through the soil. The values of the peak force were relatively similar regardless of post behavior, as reported in Table 2. However, the deeper embedded posts, which fractured, did not provide resistive forces for as long of a duration as the posts that rotated through the soil, as seen in Figure 27. As a result, the posts that fractured absorbed noticeably less energy than the posts that rotated through the soil.



Figure 26. Comparison of Post Fractures, Test Nos. SYPW-1 (Left) and SYPW-4 (Right)

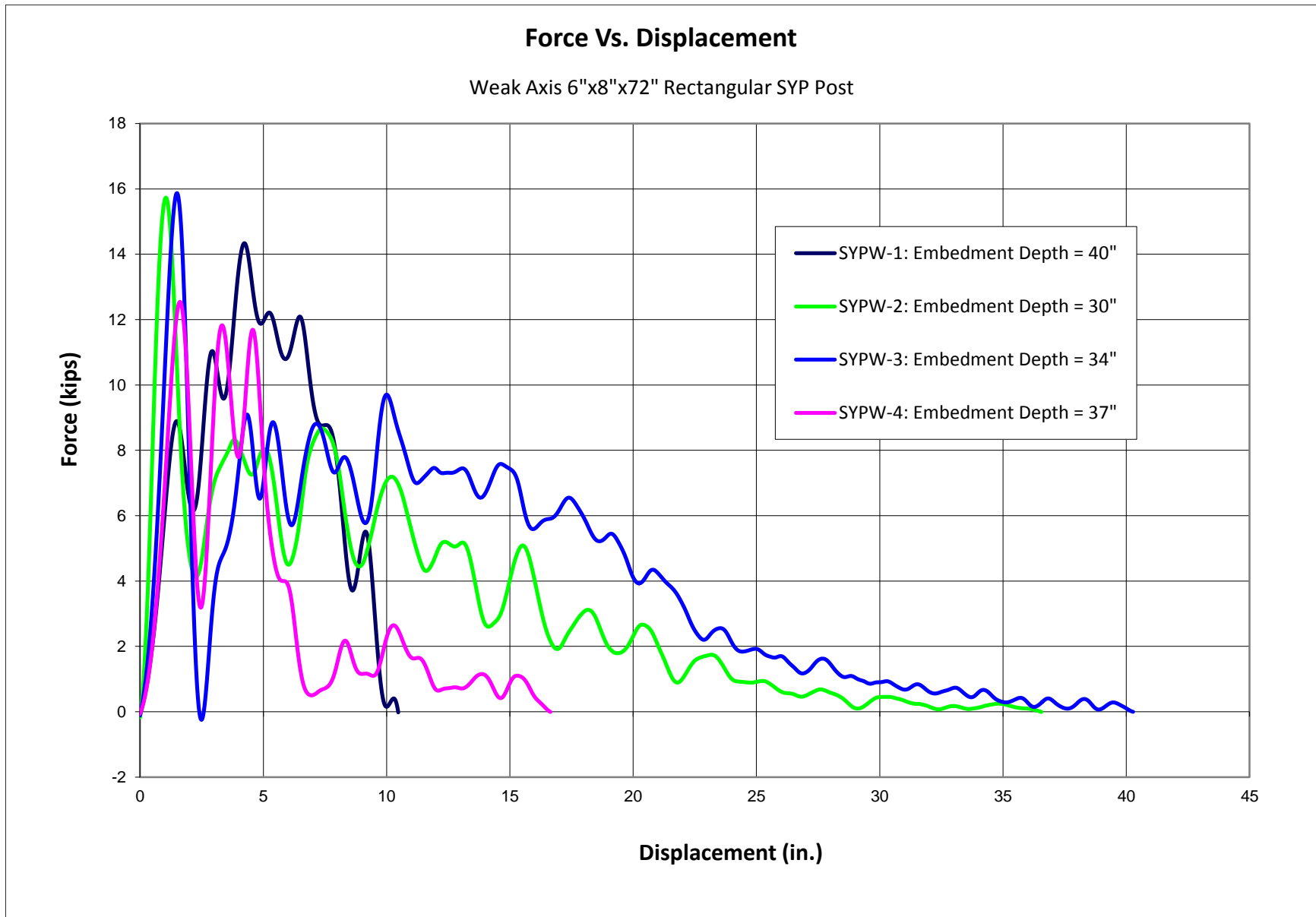


Figure 27. Force vs. Deflection Comparison, Test Nos. SYPW-1 through SYPW-4

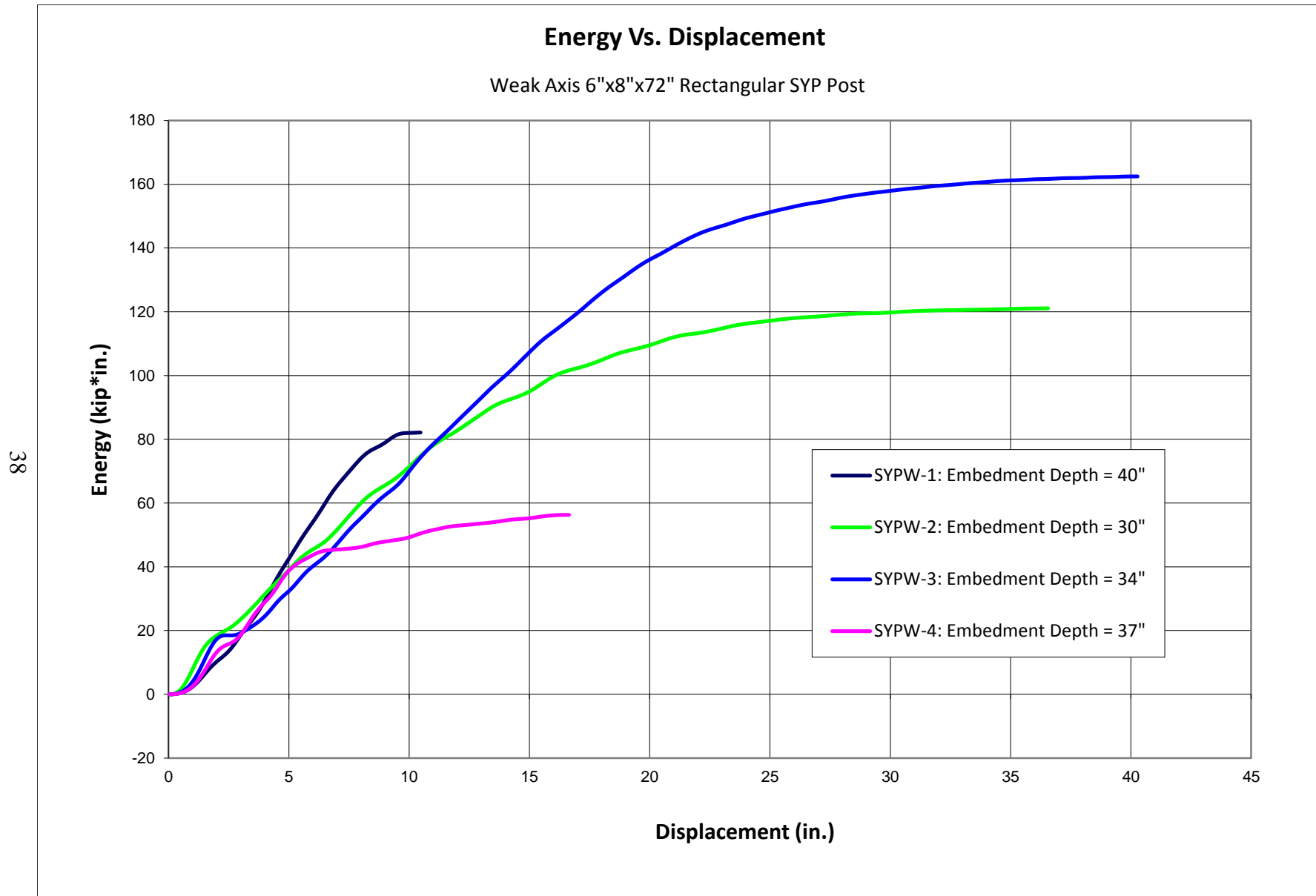


Figure 28. Energy vs. Deflection Comparison, Test Nos. SYPW-1 through SYPW-4

4 SUMMARY, CONCLUSIONS, AND RECOMMENDATIONS

The primary objective of this research study was to determine the soil-post impact reaction of W6x8.5 (W150x12.6) steel posts and 6-in. x 8-in. (152-mm x 203-mm) SYP posts along the weak axis. The study was composed of a total of five bogie tests on W6x8.5 (W150x12.6) steel posts embedded at depths ranging from 24 to 40 in. (610 to 1,016 mm), and four bogie tests conducted on 6-in. x 8-in. (152-mm x 203-mm) SYP posts embedded at depths ranging from 30 to 40 in. (762 to 1,016 mm). All posts were impacted along the weak axis.

The SYP post systems with embedment depths of 34 and 30 in. (864 and 762 mm), followed by the steel W6x8.5 (W150x12.6) post systems with embedment depths of 40 and 34 in. (1016 and 864 mm), produced the greatest energy dissipations of 162.5, 121.1, 110.1 and 113.1 kip-in. (18.4, 13.7, 12.4 and 12.8 kJ), respectively. Force vs. displacement and energy vs. displacement graphs with all nine bogie tests aggregated together are shown in Figures 29 and 30, respectively. The post systems that absorbed the most energy among the nine tests were 6-in. x 8-in. (152-mm x 203-mm) SYP posts at 30 and 34 in. (762 and 864 mm) embedment depths. These posts rotated through the soil without fracturing. However, the W6x8.5 (W150x12.6) steel post systems with embedment depths of 40 and 34 in. (1016 and 864 mm) absorbed the most energy among the steel post systems. These embedment depths allowed the post to yield and provided more energy absorption than the steel post systems that rotated through the soil.

In summary, the wood post systems absorbed more energy when rotation through the soil was witnessed compared to the wood post systems that fractured. However, the steel post system absorbed more energy when the post yielded compared to when the steel post rotated through the soil.

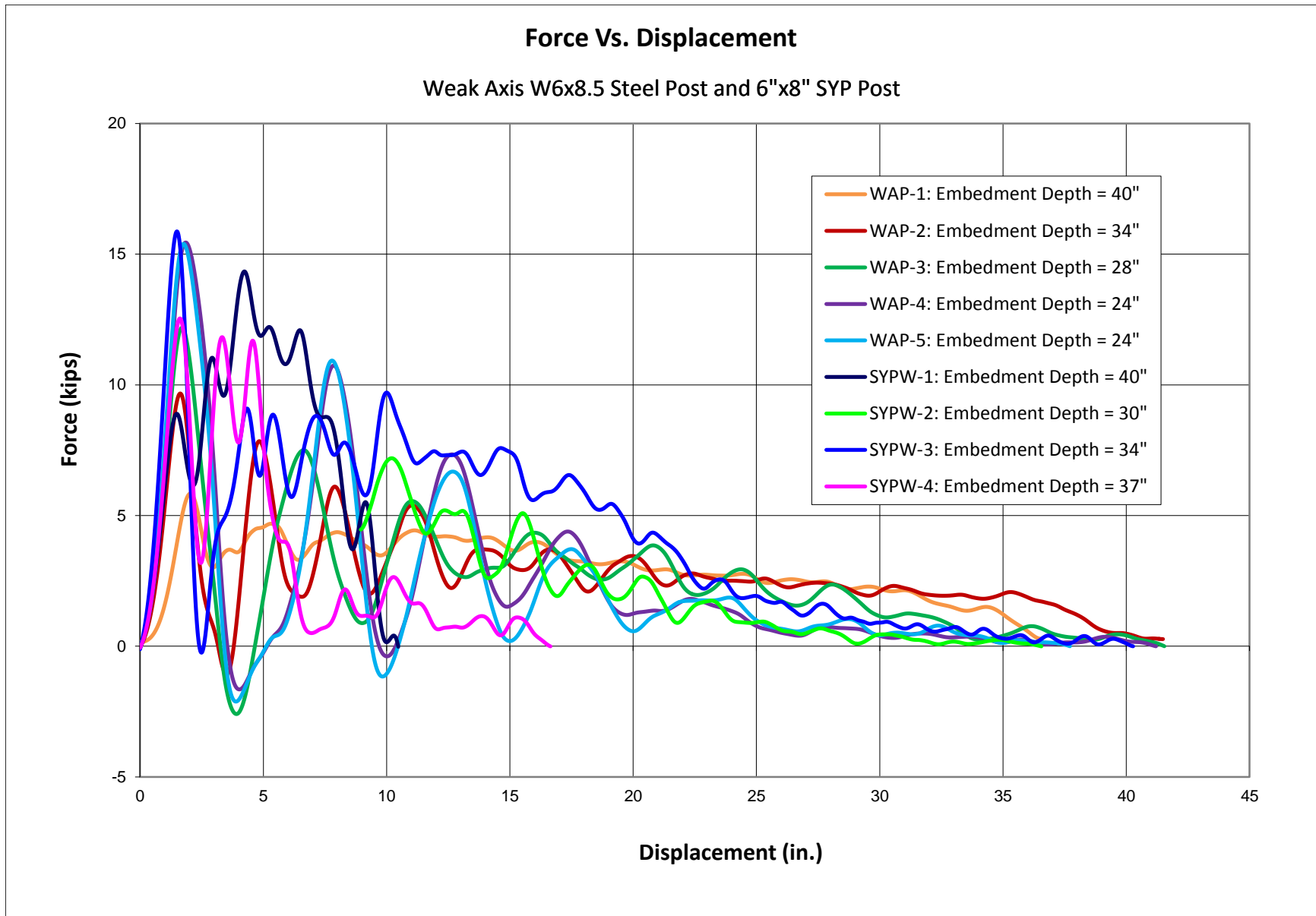
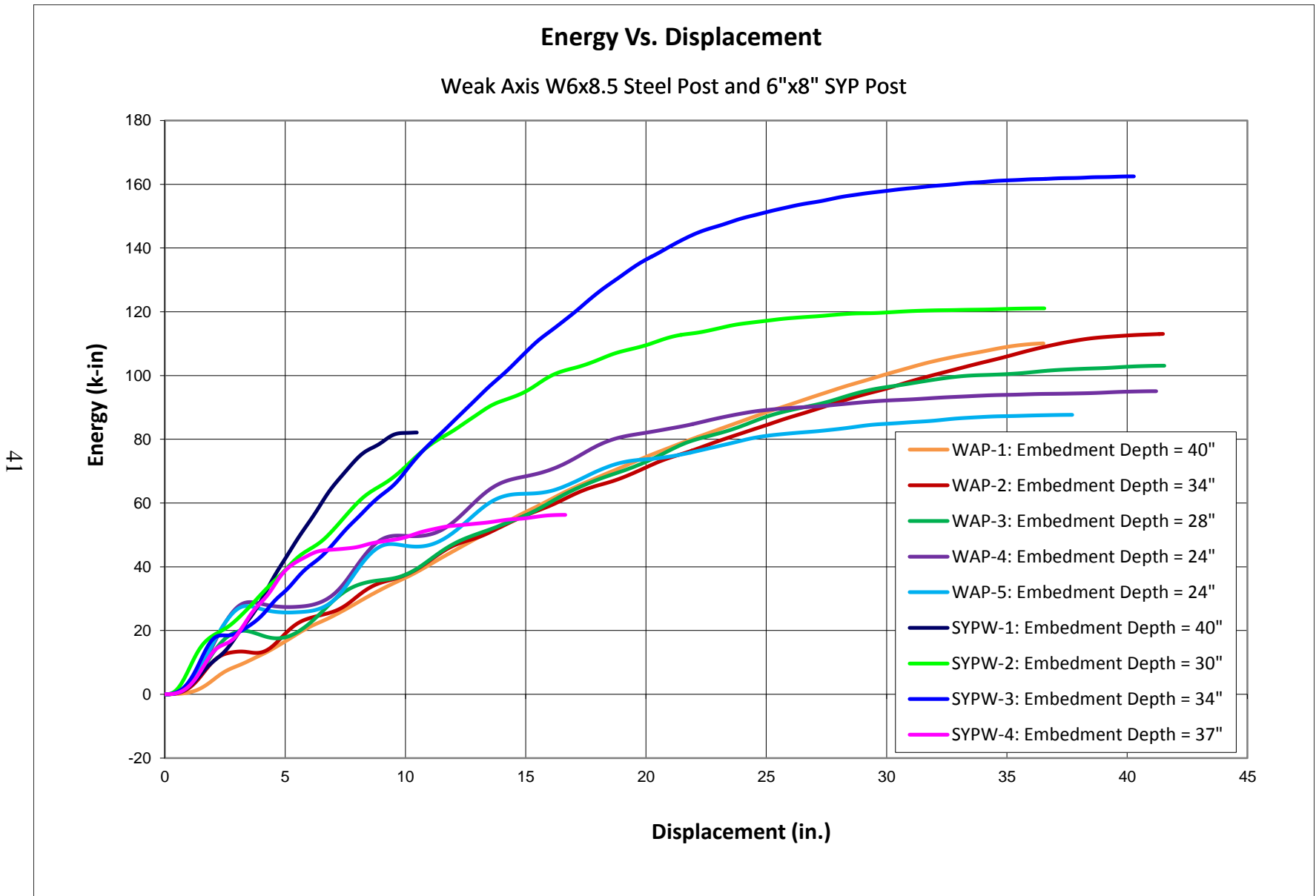


Figure 29. Combined Force vs. Deflection Comparison, All Bogie Tests



41

Figure 30. Combined Energy vs. Deflection Comparison, All Bogie Tests

5 REFERENCES

1. *Manual for Assessing Safety Hardware (MASH)*, American Association of State Highway and Transportation Officials (AASHTO), Washington, D.C., 2009.
2. Society of Automotive Engineers (SAE), *Instrumentation for Impact Test – Part 1 – Electronic Instrumentation*, SAE J211/1 MAR95, New York City, NY, July, 2007.

6 APPENDICES

Appendix A. Material Specifications

W6x8.5 R#14-0097 Red Paint
September 2013 SMT



P.O. BOX 358
GLASTONBURY, CT 06033

CERTIFICATE OF COMPLIANCE/ANALYSIS REPORT

SOLD TO:

MIDWEST MACHINERY & SUPPLY
P.O. BOX 703
Milford, NE, USA

SHIP TO:

MIDWEST MACHINERY & SUPPLY
974 238TH ROAD
MILFORD

INVOICE / S.O.: 0172110 / 0116560
CUSTOMER P.O.: 2795

REFERENCE: STOCK
DATE SHIPPED: 08/08/13

QTY:	HEAT/LOT NO:	ITEM NUMBER:	YIELD:	CC:	TENSILE:	%ELONG:	DESCRIPTION:						
							C:	Mn:	P:	S:	Si:	Cl:	Type
850 (350)	55028671	T-POG060080600		IB-B0600800			THRIE POST W06 x 008.5# x 06'00 GALV						
(500)	55028670			IB-B0600800									

ALL STEEL USED IN MANUFACTURING IS MADE AND MELTED IN THE USA, INCLUDING HARDWARE FASTENERS, AND COMPLIES WITH THE BUY AMERICA ACT. ALL COATINGS PROCESSES ARE PERFORMED IN THE USA AND COMPLY WITH THE BUY AMERICA ACT. BOLTS COMPLY WITH ASTM A-307 SPECIFICATIONS AND ARE GALVANIZED IN ACCORDANCE WITH ASTM-153, UNLESS OTHERWISE STATED. NUTS COMPLY WITH ASTM-563 SPECIFICATIONS AND ARE GALVANIZED IN ACCORDANCE WITH ASTM-153 UNLESS OTHERWISE STATED. **WASHERS COMPLY WITH ASTM F-436 AND/OR F-844 SPECIFICATIONS** AND ARE GALVANIZED IN ACCORDANCE WITH ASTM-153 UNLESS OTHERWISE STATED. ALL GUARDRAIL MEETS AASHTO M-180, AND ALL STRUCTURAL STEEL MEETS AASHTO M-270. ALL OTHER GALVANIZED MATERIAL CONFORMS WITH ASTM-123. ALL OTHER ITEMS COMPLY WITH AASHTO M-111, M-165, M-133, M-265, ASTM A36, ASTM-709, ASTM-123, ASTM A505, AND ASTM588 SPECIFICATIONS IF APPLICABLE. COMPLIANCE WITH ALL SPECIFICATIONS OF DEPARTMENT OF PUBLIC WORKS, DEPARTMENT OF HIGHWAYS AND TRANSPORTATION, DIVISION OF ROADS AND BRIDGES AND STATE HIGHWAY ADMINISTRATION IS MET IN ALL RESPECTS.

HIGHWAY SAFETY CORPORATION

QUALITY ASSURANCE MANAGER

NOTARIZED UPON REQUEST:
STATE OF CONNECTICUT COUNTY OF HARTFORD
SWORN AND SUBSCRIBED BEFORE ME THIS

14 DAY OF August, 20 13

Notary Public

MARGARET J. SATALINO
NOTARY PUBLIC
MY COMMISSION EXPIRES OCT. 31, 2016

Figure A-1. Material Specifications, W6x8.5 (W150x12.6) Steel Post, Test Nos. WAP-1 through WAP-5



US-ML-CARTERSVILLE
 384 OLD GRASSDALE ROAD NE
 CARTERSVILLE, GA 30121
 USA

CERTIFIED MATERIAL TEST REPORT

CUSTOMER SHIP TO HIGHWAY SAFETY CORP 473 W FAIRGROUND ST MARION, OH 43302-1701 USA		CUSTOMER BILL TO HIGHWAY SAFETY CORP GLASTONBURY, CT 06033-0358 USA		GRADE A992/A709-36	SHAPE / SIZE Wide Flange Beam / 6 X 8.5#	
SALES ORDER 448220/000020		CUSTOMER MATERIAL N°		LENGTH 42'00"	WEIGHT 37,485 LB	HEAT / BATCH 55028671/02
CUSTOMER PURCHASE ORDER NUMBER 001562143 IB-B0600800			BILL OF LADING 1323-0000008317	DATE 07/17/2013		
SPECIFICATION / DATE or REVISION 1-ASTM A6/A6M-11 2-A992/A992M-11 3-A709/A709M-11 4-A36/A36M-08						

CHEMICAL COMPOSITION													
C	Mn	P	S	Si	Cu	Ni	Cr	Mo	V	Nb	N	Pb	
%	%	%	%	%	%	%	%	%	%	%	%	%	%
0.14	0.90	0.015	0.020	0.19	0.29	0.10	0.07	0.034	0.016	0.002	0.0090	0.0080	

CHEMICAL COMPOSITION	
Sn	%
0.012	

MECHANICAL PROPERTIES						
Elong.	G/L	UTS	UTS	YS 0.2%	YS	
%	Inch	PSI	MPa	PSI	MPa	
20.20	8.000	74300	512	50900	351	
22.10	8.000	74000	510	54800	378	

COMMENTS / NOTES

The above figures are certified chemical and physical test records as contained in the permanent records of company. This material, including the billets, was melted and manufactured in the USA. CMTR complies with EN 10204 3.1.

Bhaskar
 BHASKAR YALAMANCHILI
 QUALITY DIRECTOR

YAN WANG
 QUALITY ASSURANCE MGR.

46

Figure A-2. Material Specifications, W6x8.5 (W150x12.6) Steel Post, Test Nos. WAP-1 through WAP-5

Qsmosee®
 Pressure
 Treated Lumber



LUMBER COMPANY, INC.
 P.O. BOX 99 - 285 SIKE STOREY ROAD - ARMUCHEE, GA 30105
 706-234-1605 www.sistoreylumber.com

20254

SISTOREY
 154 Date 07/20/10

S Midwest Machinery & Supply
 P.O. Box 81097
 D Lincoln, NE 68501
 T
 O

D Midwest Machinery & Supply
 E 1-80 Exit 382
 L Milford, NE
 T
 O

CUST. ORD. NO. 2333		DEL. BY: MTW/SE Logistics	SOLD BY: CRC	ORD. BY: Ray Schact		
Pieces	Description	Total Feet	Price	Amount		
1	KS Dot Timber Guardrail Components #1 SYP Grade	Marked;	Q.M.	\$4S;	.60CCA	
2	42 6 x 8 - 6'6" Line Post					
3	168 6 x 8 - 6'6" Rub Post					
4	42 6 x 8 - 6'6" CRT Post					
5	168 6 x 8 - 0'14" Blockout (C.D.)					
6	168 6 x 8 - 0'23" Rub Block (C.D.)					
7	36 6 x 8 x 0'23" Rub Block (Routed)					
8	NE DOR Timber Guardrail Components					
9	105 6 x 8 - 6' Line Post					
10						
11						
12	Paint Charge numbers on bundles					
13	T/R and CoC with Invoice and Mailed to:					
14	Mike Popp, Kansas DOT; Materials Lab, Bldg 1,					
15	3200 45th St. North, Wichita, KS 67220					
16	Nebraska DOR Timber Guardrail Components;					
17	#1 SYP Dense (except blocks), RGH; .60CCA					
18	Paint Charge numbers on bundles					
19	T/R and CoC with TRUCK					
20	Customer Contact: Ray Schact @ 402-761-3262					
21						
22						
23						
24	13 bundles					
25						
26						
27						
28						

TERMS NET 30 - due 8/19/10

A service charge of 1½% per month, equal to 18% annually, will be charged on all past due accounts.

If any dispute arises from or is related to the purchase of any goods, products, lumber or services from Seller or if Seller finds it necessary to initiate a lawsuit for the collection of any amount owing to Seller arising from the sale of any goods, products, lumber or services, then the Purchaser and Seller do hereby expressly consent to the jurisdiction and venue of the State Courts of Floyd County, Georgia.

Received the above in good condition

REC'D BY

South East Coast *Ray Schact*

THANK YOU

Please Keep This Copy For Your Reference

Figure A-3. Material Specifications, 6-in. x 8-in. (152-mm x 203-mm) SYP Post, Test Nos.

SYPW-1 through SYPW-4



CERTIFICATE OF COMPLIANCE

JULY 20, 2010

MIDWEST MACHINERY & SUPPLY
MILFORD, NE

THE FOLLOWING MATERIAL DELIVERED ON 7/20/10 ON BILL OF LADING NUMBER 20254 HAS BEEN INSPECTED BEFORE AND AFTER TREATMENT AND IS IN FULL COMPLIANCE WITH APPLICABLE NEBRASKA DEPARTMENT OF ROADS REQUIREMENTS FOR SOUTHERN YELLOW PINE TIMBER GUARDRAIL COMPONENTS, PRESERVATIVE TREATED WITH CHROMATED-COPPER-ARSENATE (CCA-C) TO A MINIMUM RETENTION OF .60 LBS/CU.FT. THE ACCEPTANCE OF EACH PIECE BY COMPANY QUALITY CONTROL IS INDICATED BY A HAMMER BRAND ON THE END OF EACH PIECE.

MATERIAL	CHARGE #	DATE	RETENTION	QUANTITY
6x8x6' Line Post	10-342	7/1/10	0.62	105

THIS CERTIFICATE APPLIES TO MATERIAL ORDERED FOR your order no.: 2333
FOR ANY INQUIRIES, PLEASE RETAIN THIS DOCUMENT FOR FUTURE REFERENCE.
THANK YOU FOR YOUR ORDER.

SINCERELY,

Karen Storey

SIGNED BEFORE ME THIS 20 DAY OF JULY 2010.

Notary:
Notary Public Floyd County Georgia
My Commission Expires Oct. 19, 2010



Phone: 706-234-1605

P.O. Box 99, Armuchee, GA 30105

Fax: 706-235-8132

Figure A-4. Material Specifications, 6-in. x 8-in. (152-mm x 203-mm) SYP Post, Test Nos. SYPW-1 through SYPW-4

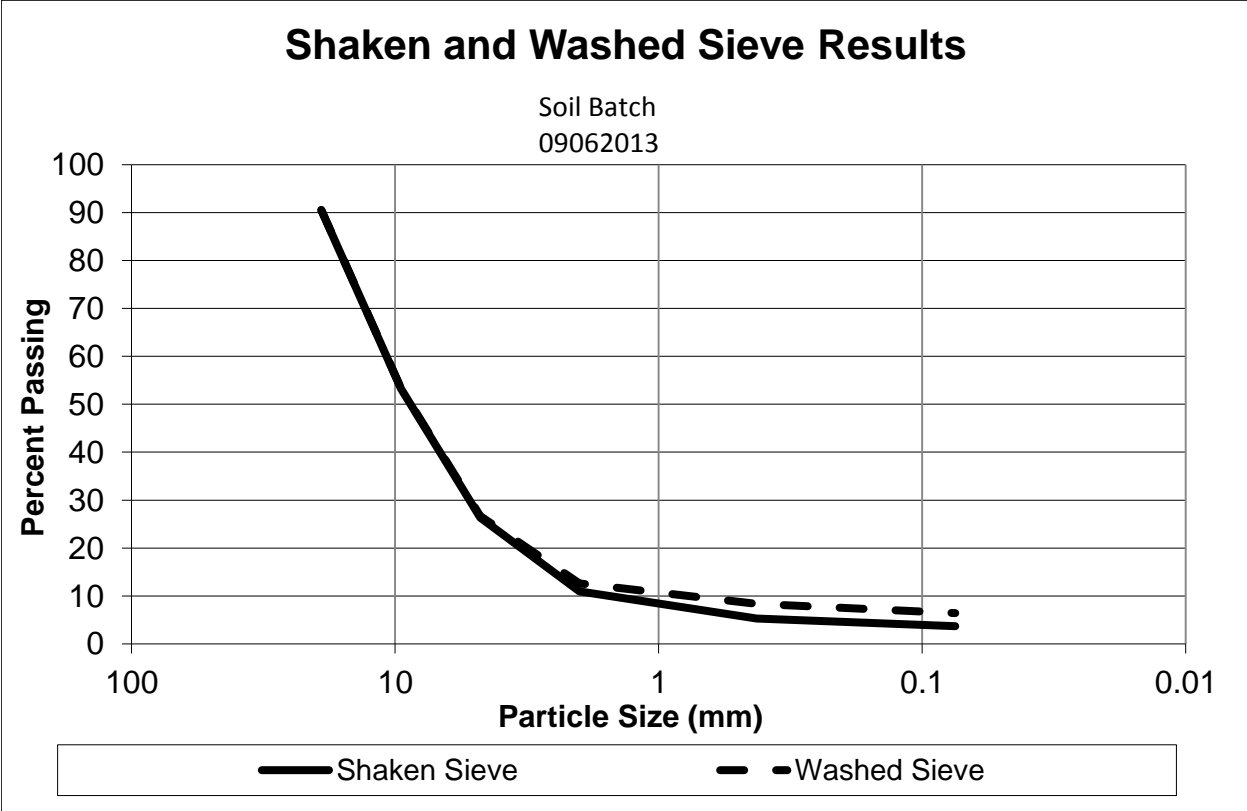


Figure A-5. Graph of Soil Sieve Data for All Bogie Tests

Appendix B. Bogie Test Results

The results of the recorded data from each accelerometer for every dynamic bogie test are provided in the summary sheets found in this appendix. Summary sheets include acceleration, velocity, and deflection vs. time plots, as well as force vs. deflection and energy vs. deflection plots.

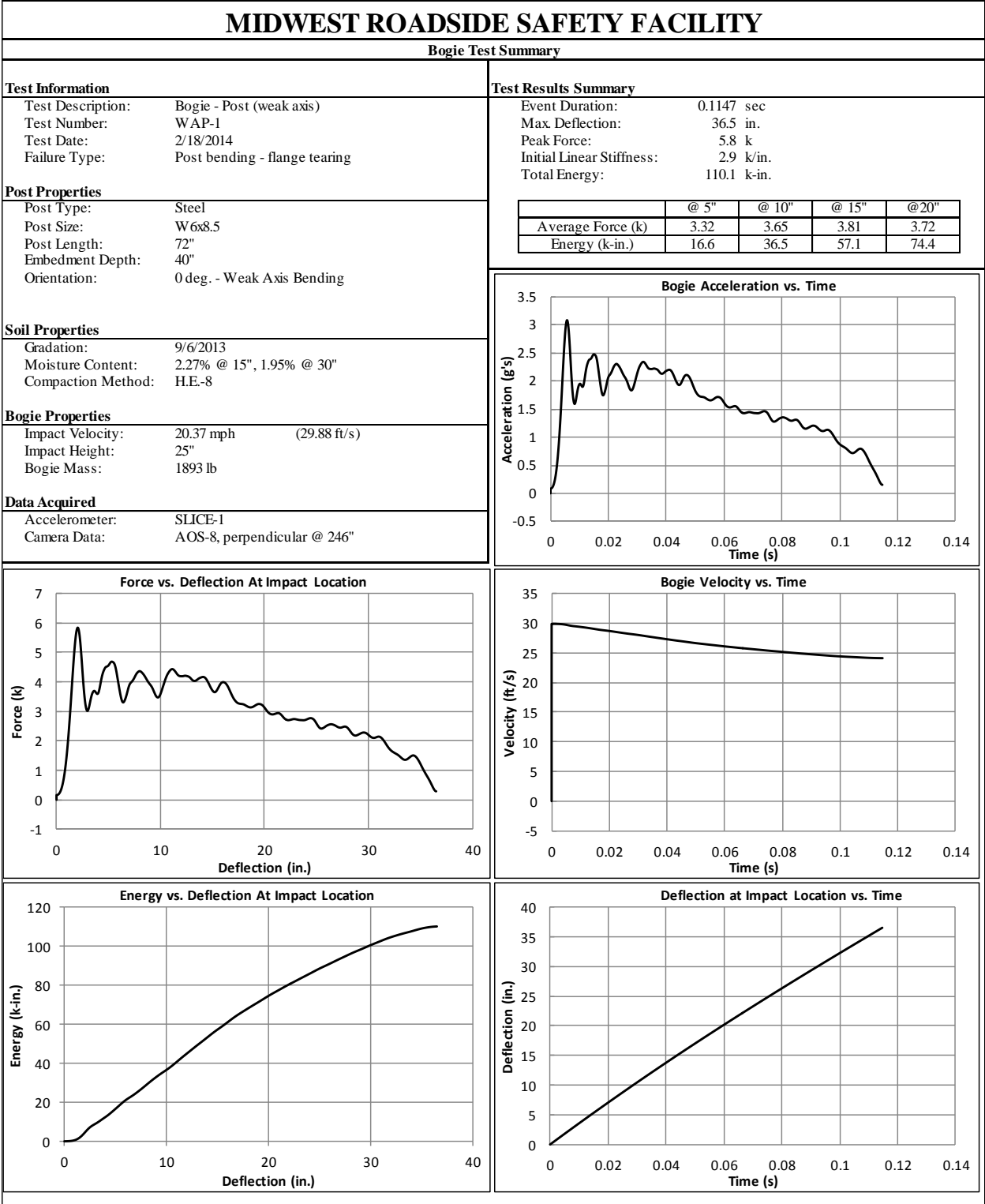


Figure B-1. Test No. WAP-1 Results (SLICE -1)

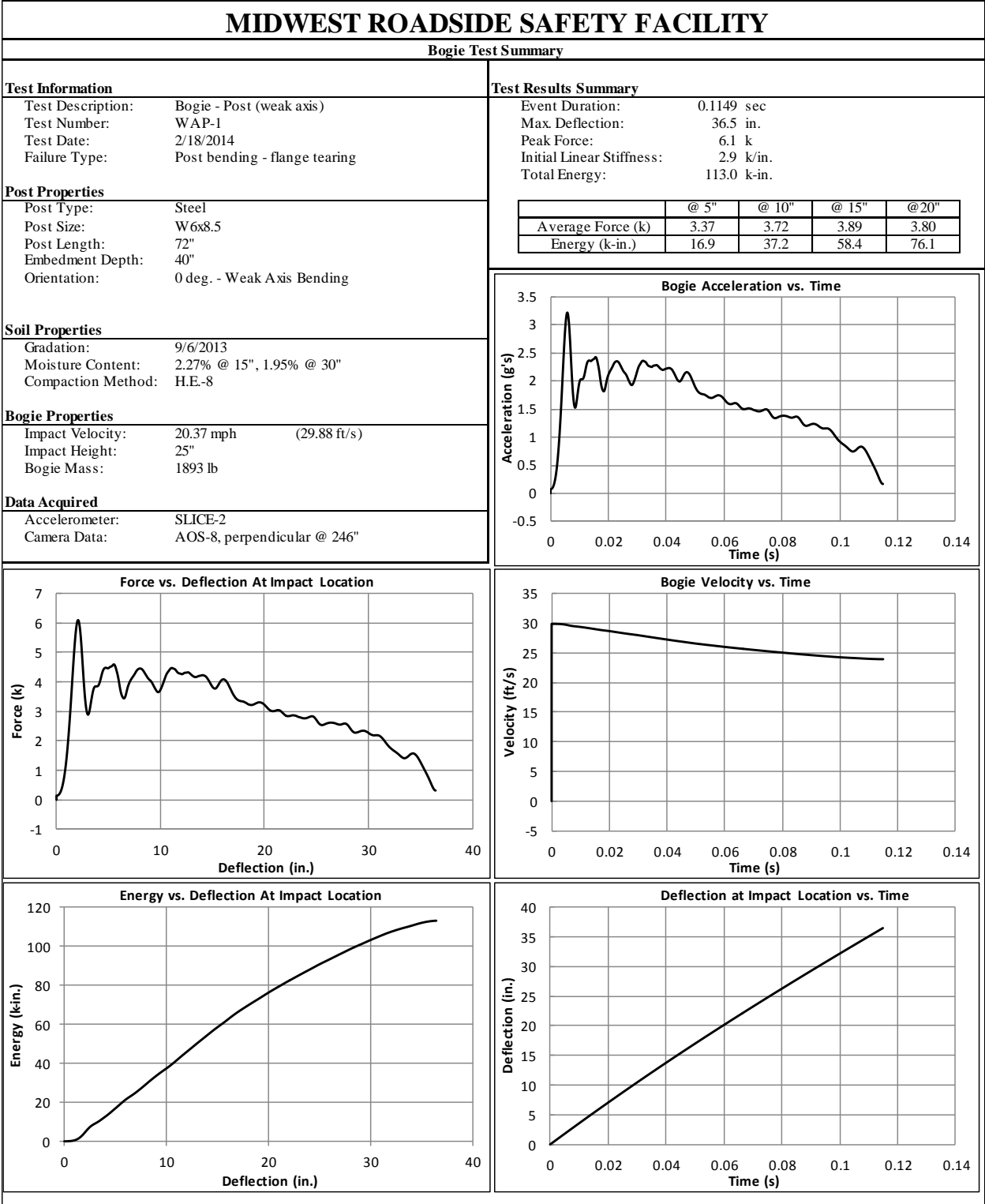


Figure B-2. Test No. WAP-1 Results (SLICE -2)

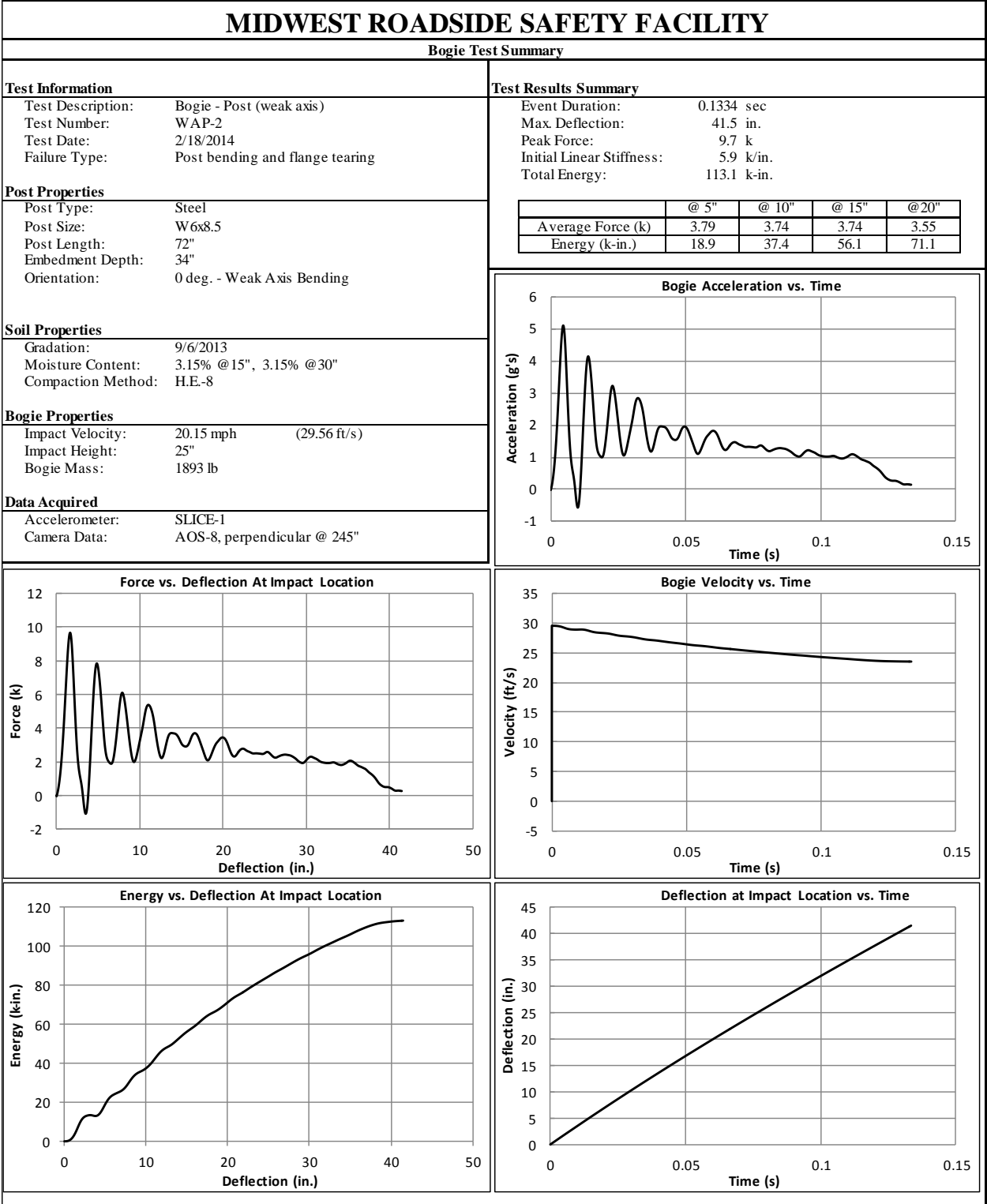


Figure B-3. Test No. WAP-2 Results (SLICE -1)

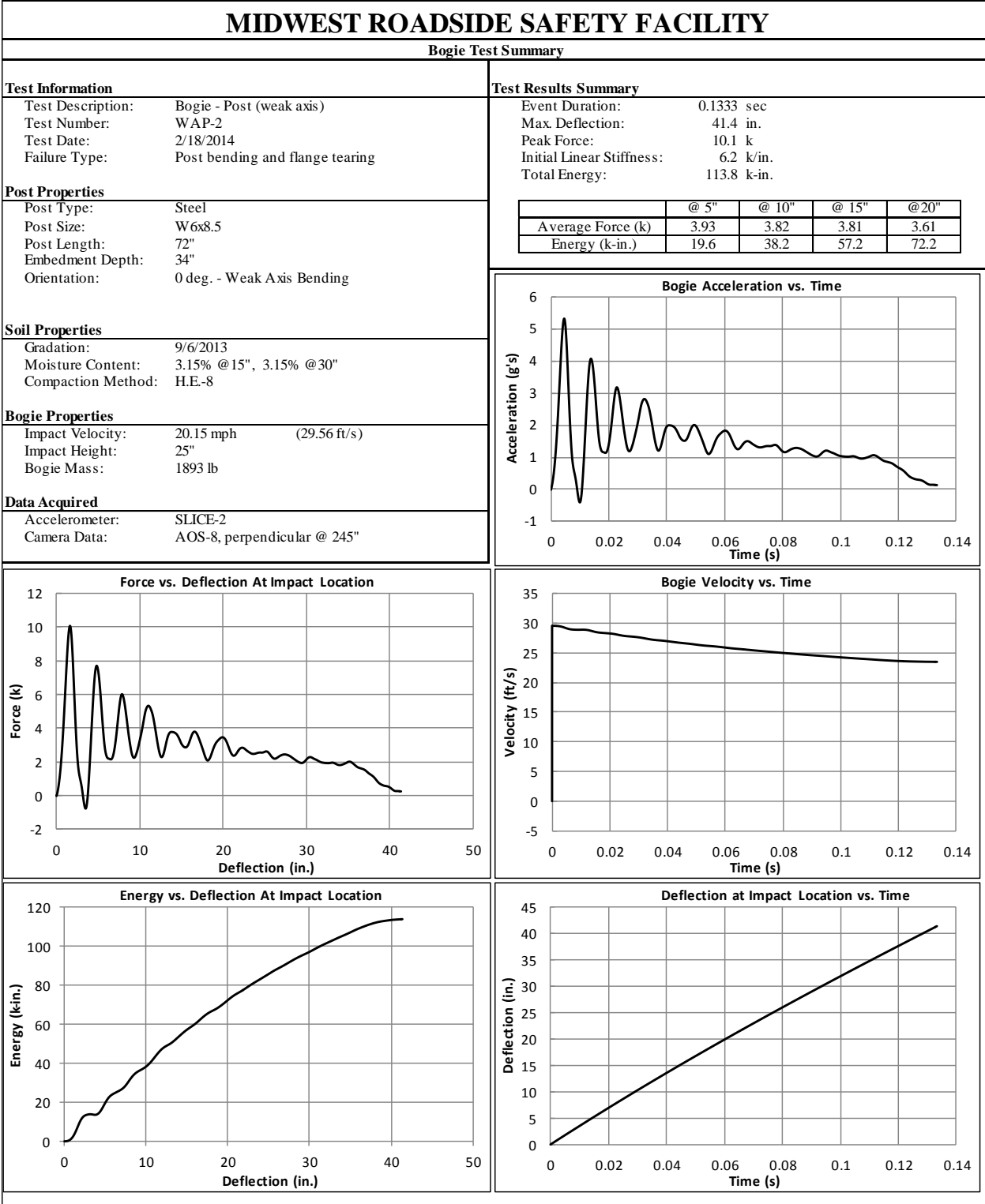


Figure B-4. Test No. WAP-2 Results (SLICE -2)

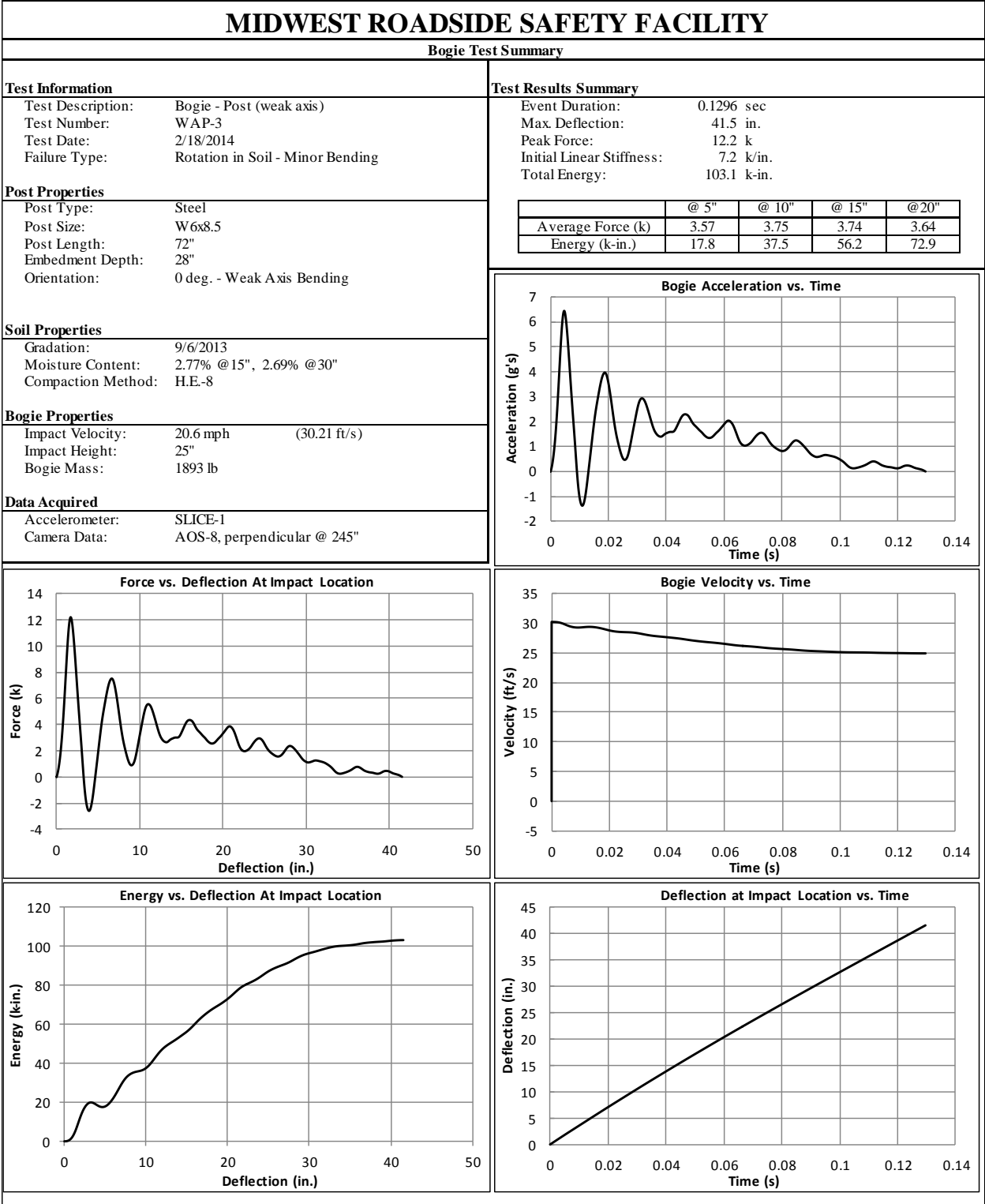


Figure B-5. Test No. WAP-3 Results (SLICE -1)

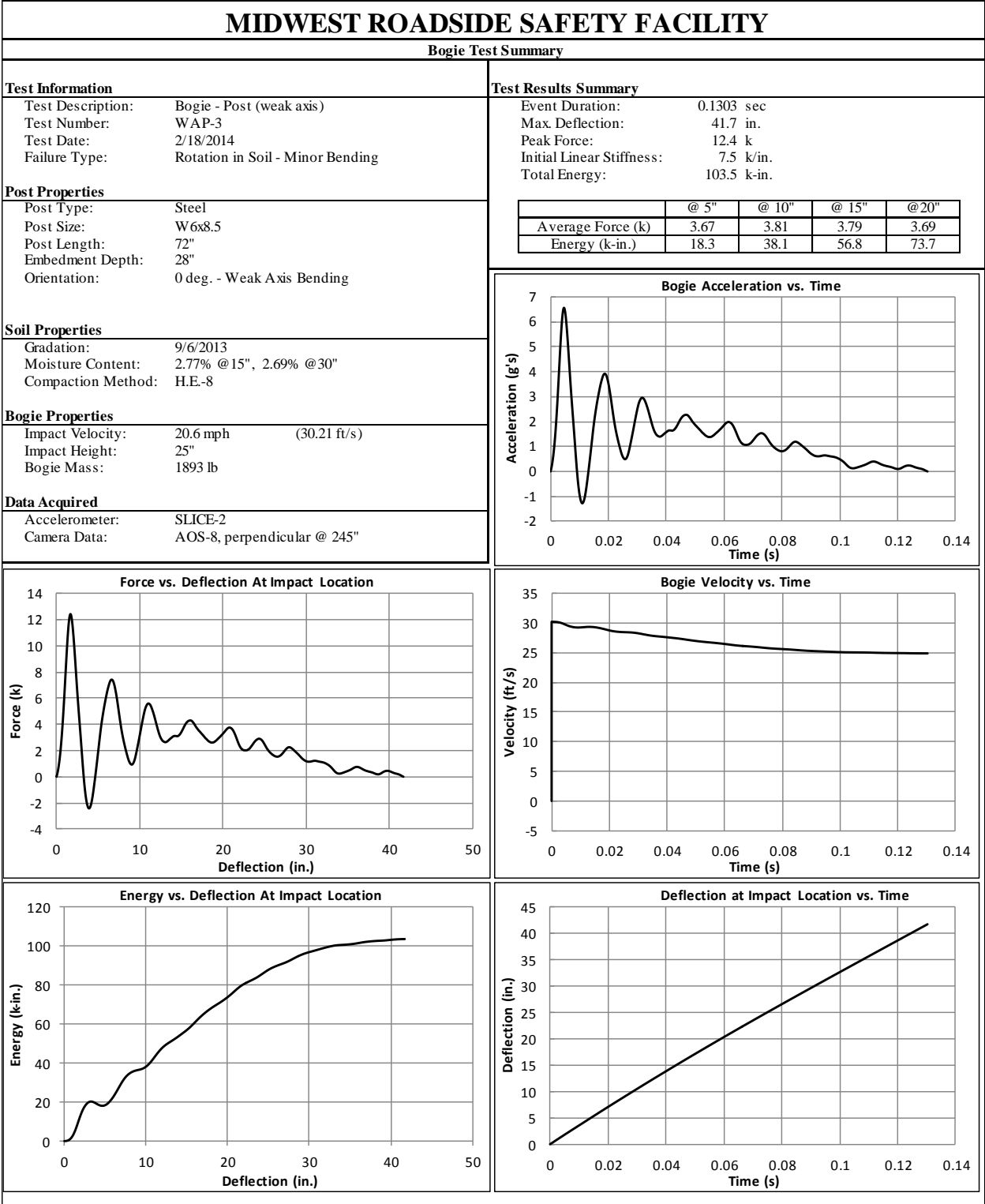


Figure B-6. Test No. WAP-3 Results (SLICE -2)

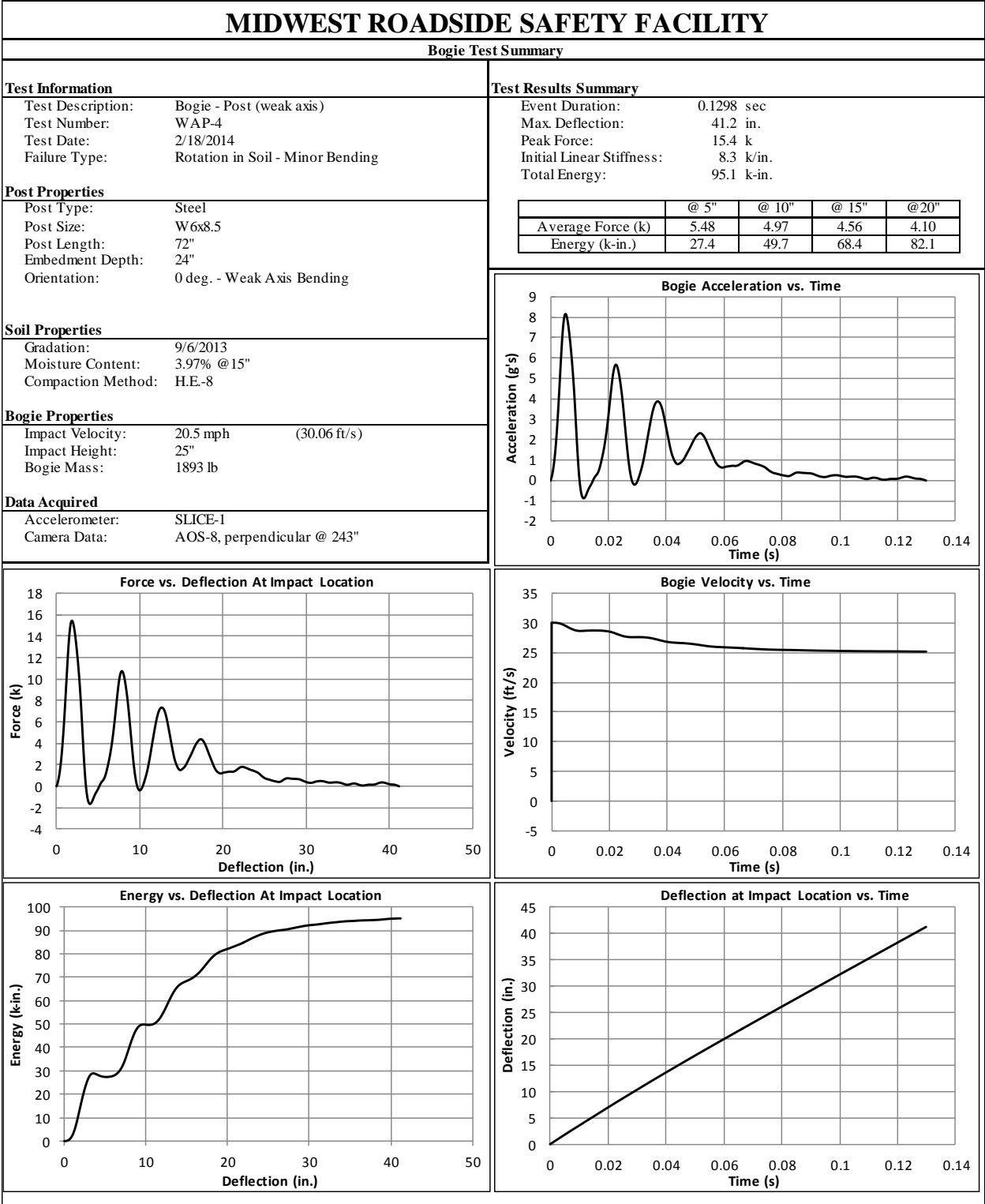


Figure B-7. Test No. WAP-4 Results (SLICE -1)

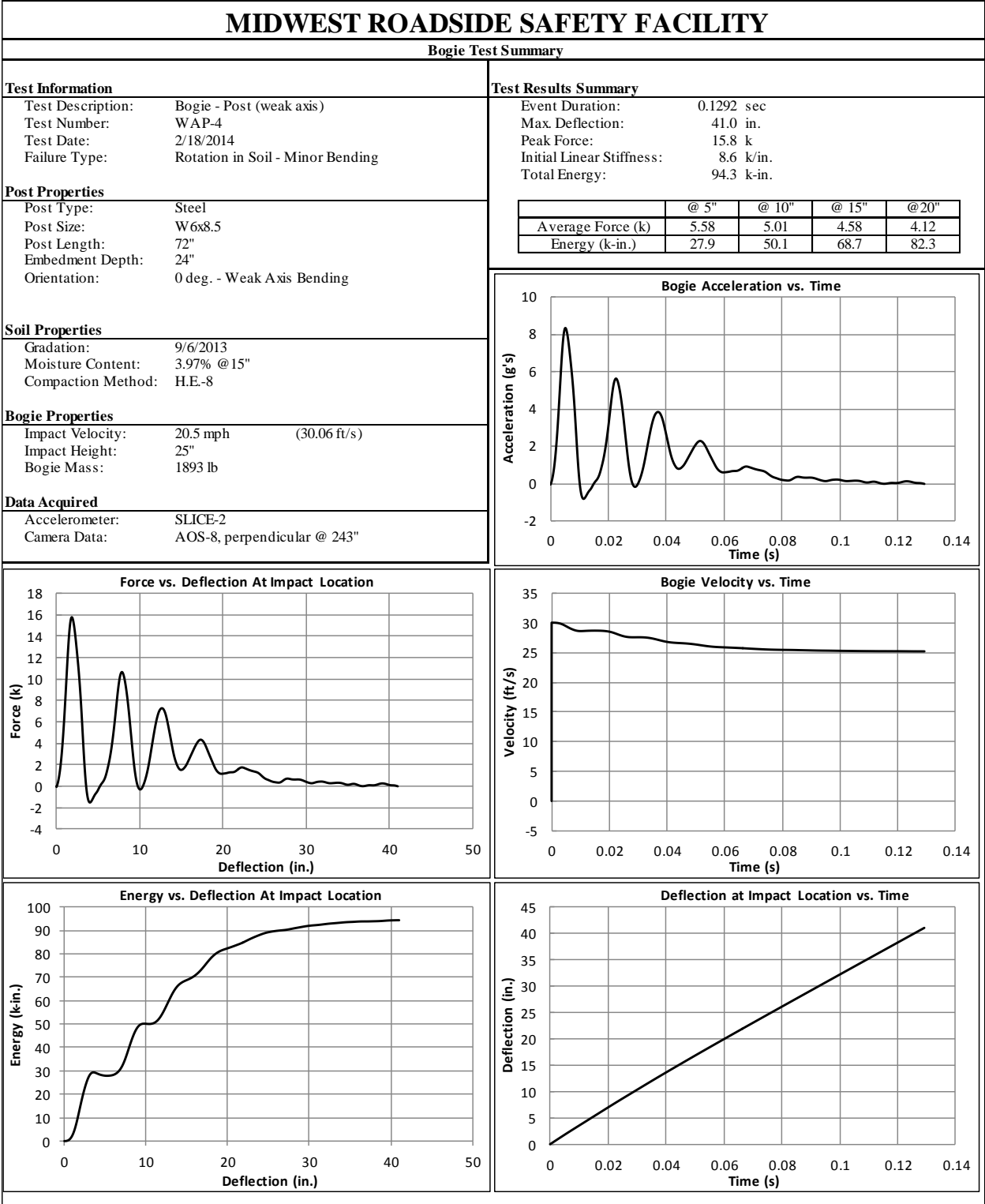


Figure B-8. Test No. WAP-4 Results (SLICE -2)

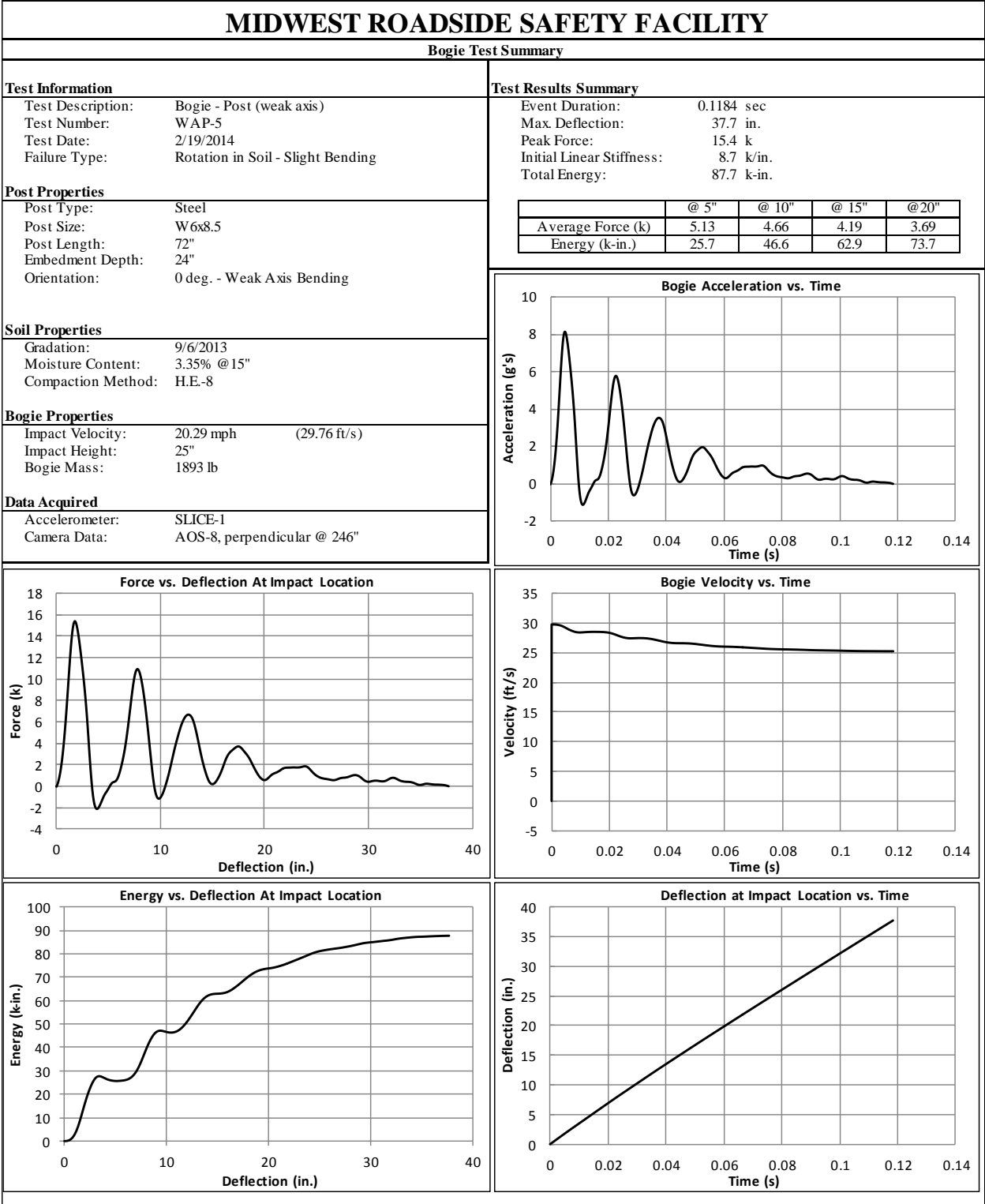


Figure B-9. Test No. WAP-5 Results (SLICE -1)

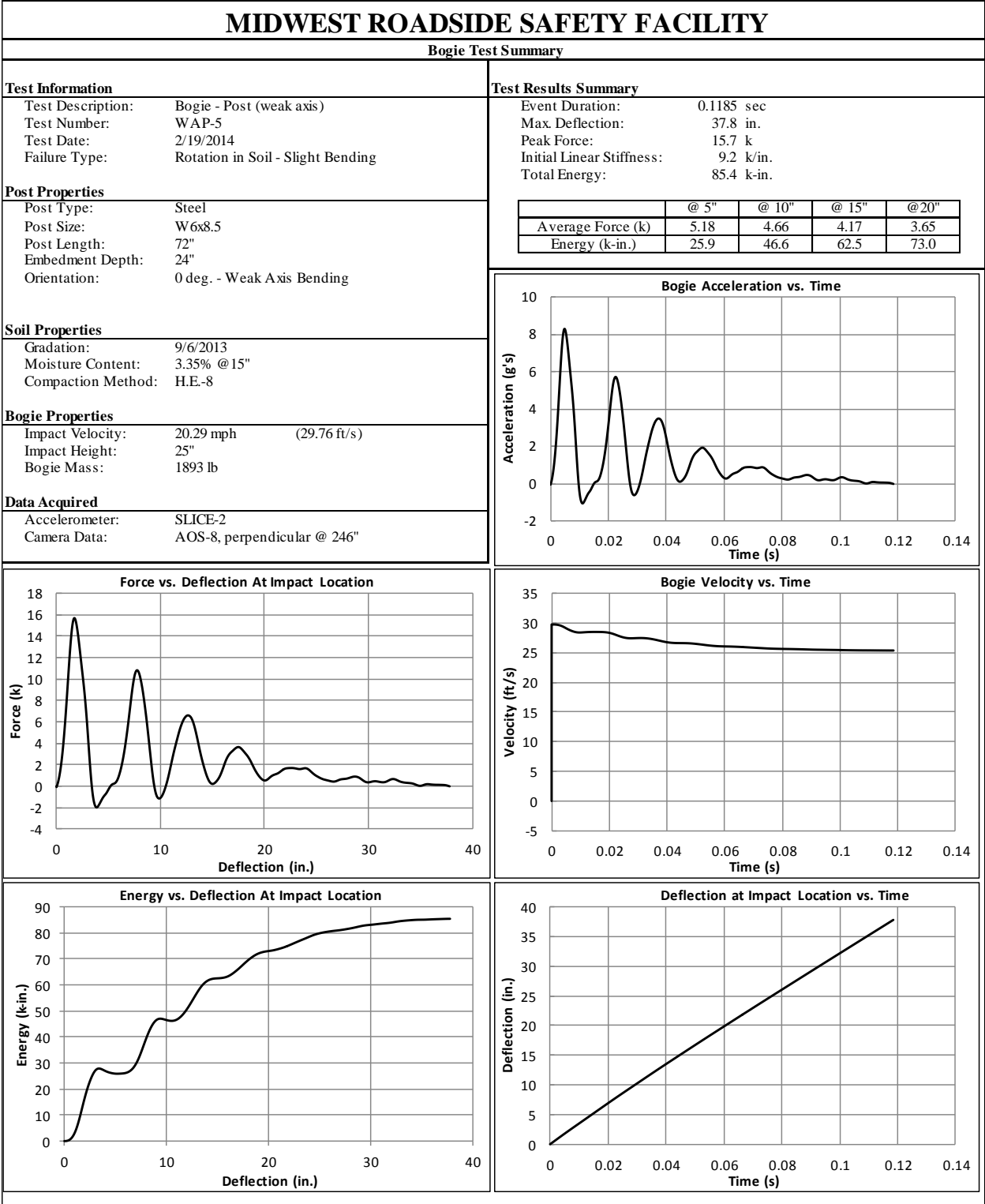


Figure B-10. Test No. WAP-5 Results (SLICE -2)

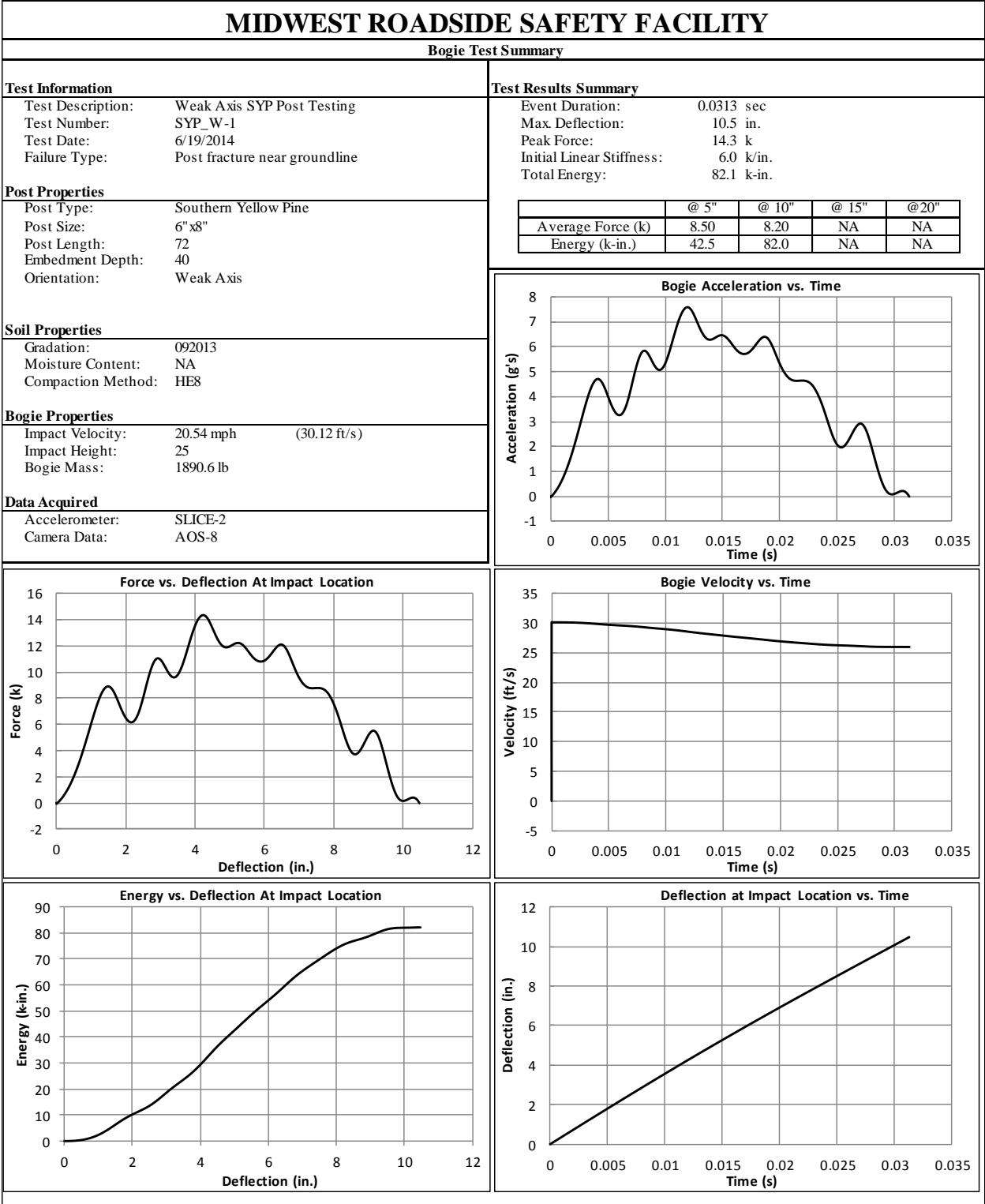


Figure B-11. Test No. SYPW-1 Results (SLICE -2)

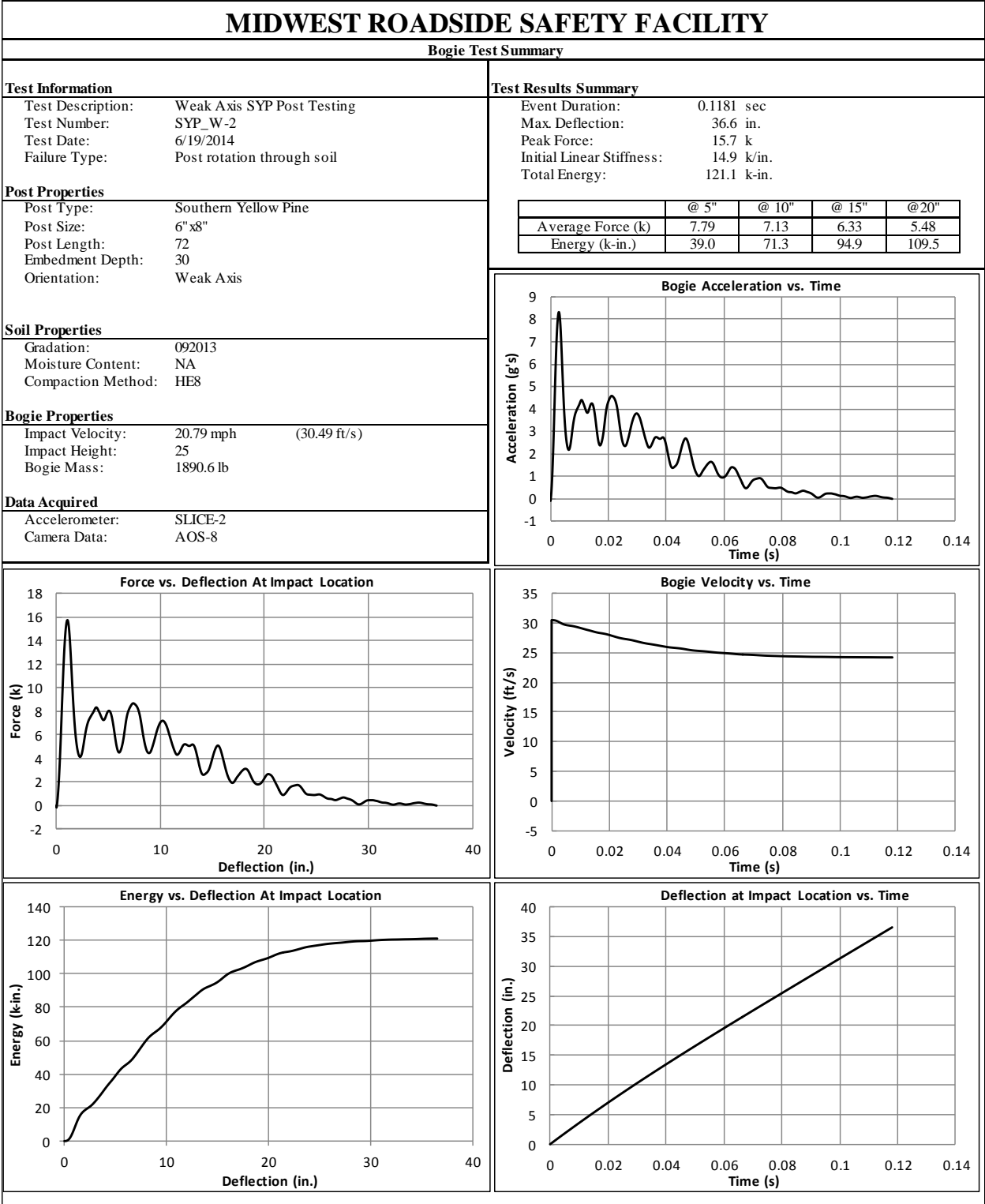


Figure B-12. Test No. SYPW-2 Results (SLICE -2)

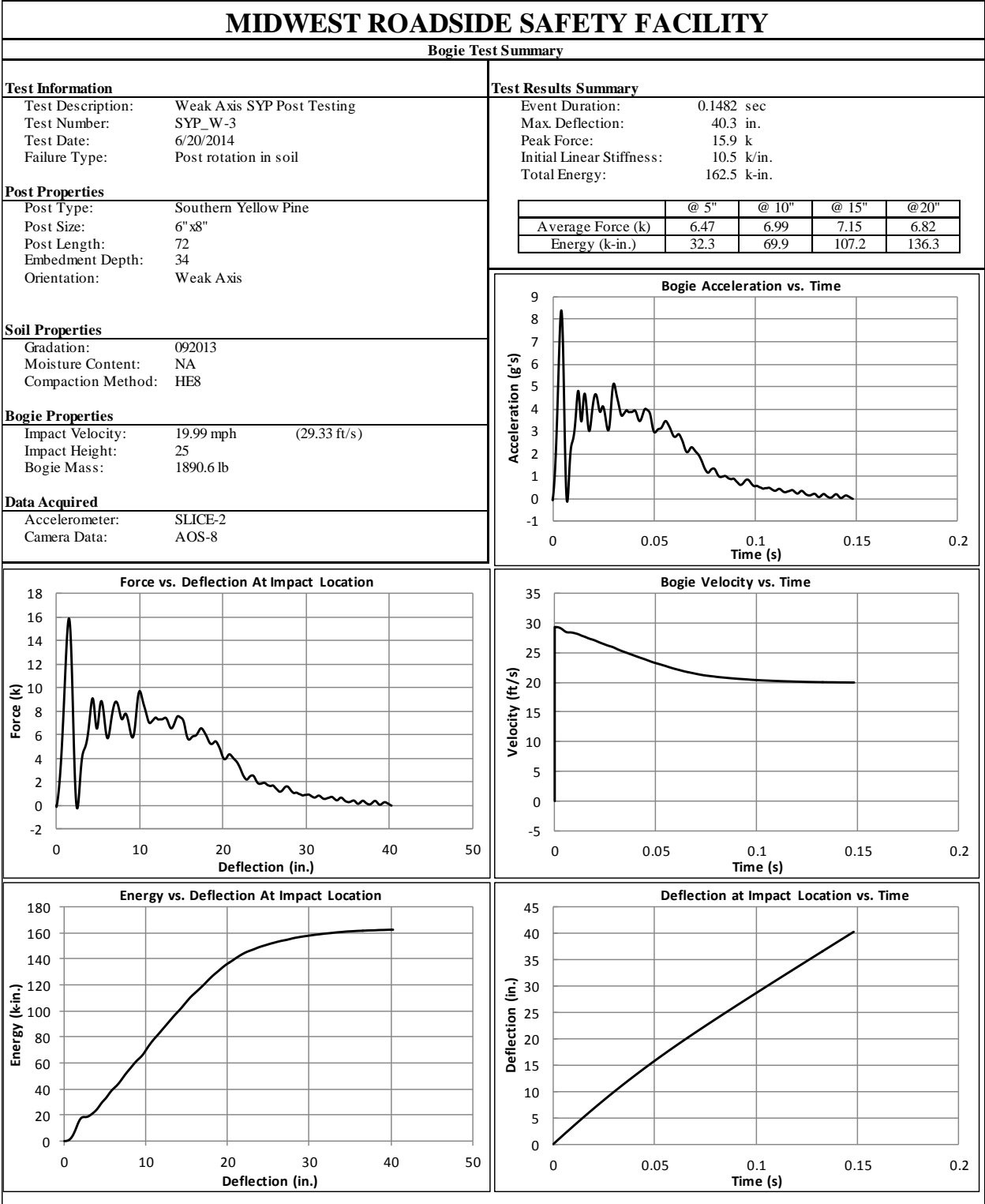


Figure B-13. Test No. SYPW-3 Results (SLICE -2)

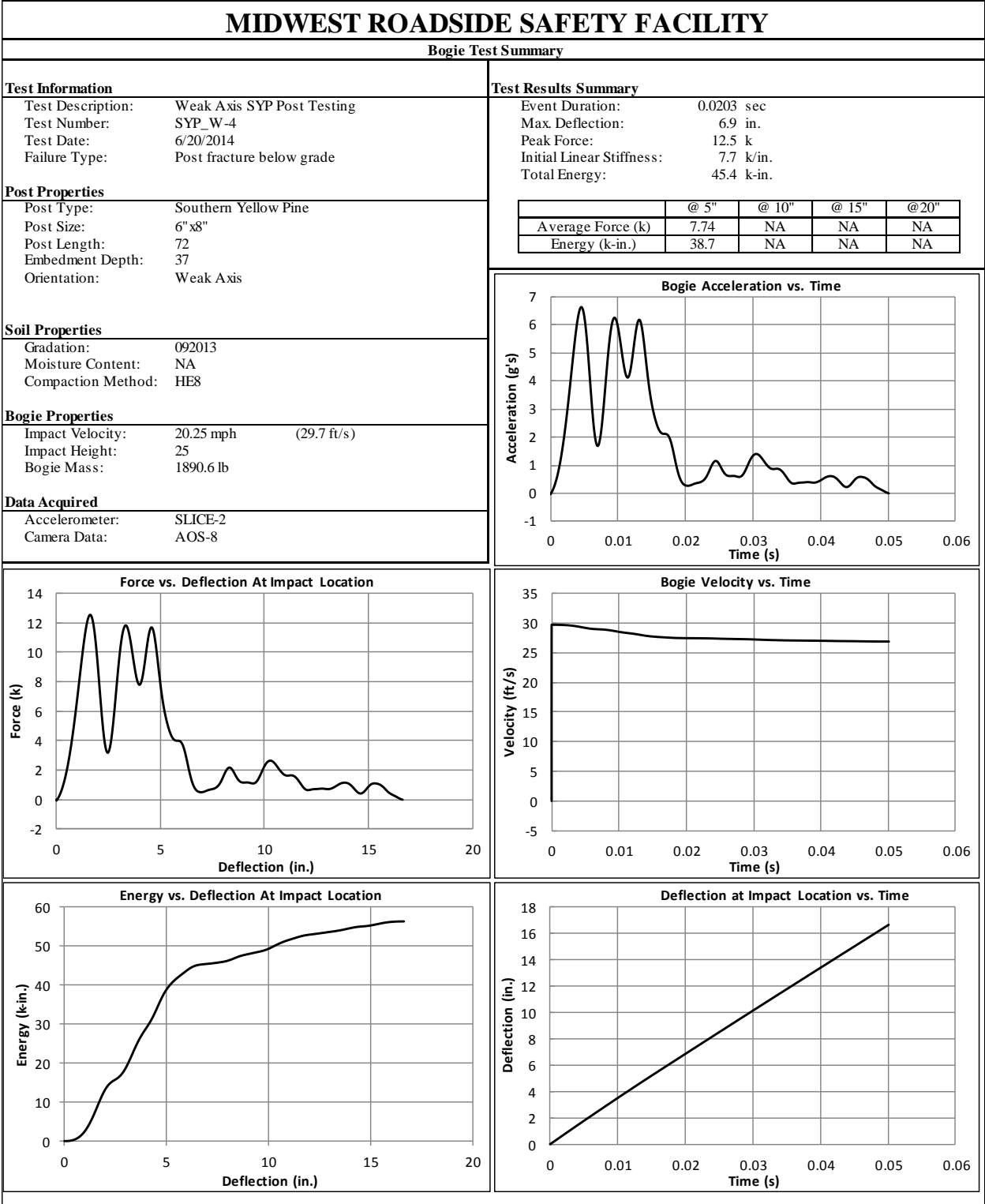


Figure B-14. Test No. SYPW-4 Results (SLICE -2)

Appendix C. SYP Post Inspection

Non-Round Post Inspection/Properties

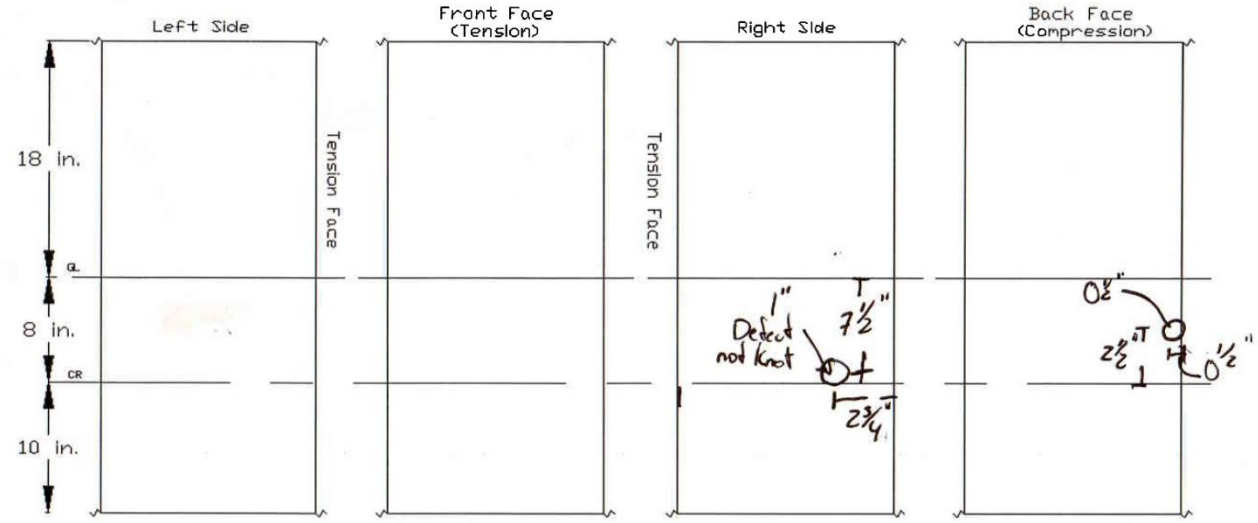
Rev. 1 (1/4/2014)

Test No.: _____

Knot/Defect Inspection Date: 6-17-14

Post 1

All dimensions are in inches.



Test Day Measurements

Date Measured: 6-18-14

Post Length: 72 3/4"

Post Weight: 63 lbs

Ring Density: 22 1/3 = 7 1/3 rings/inch

Additional Notes:

On right side the defect is a small impression

	Top	GL	CR	Bottom
Width	<u>7 3/4</u>	<u>7 3/4</u>	<u>7 3/8</u>	<u>7 3/4</u>
Depth	<u>5 3/4</u>	<u>5 1/8</u>	<u>5 1/8</u>	<u>6</u>
Moisture	<u>14</u>	<u>14</u>	<u>14</u>	<u>14</u>

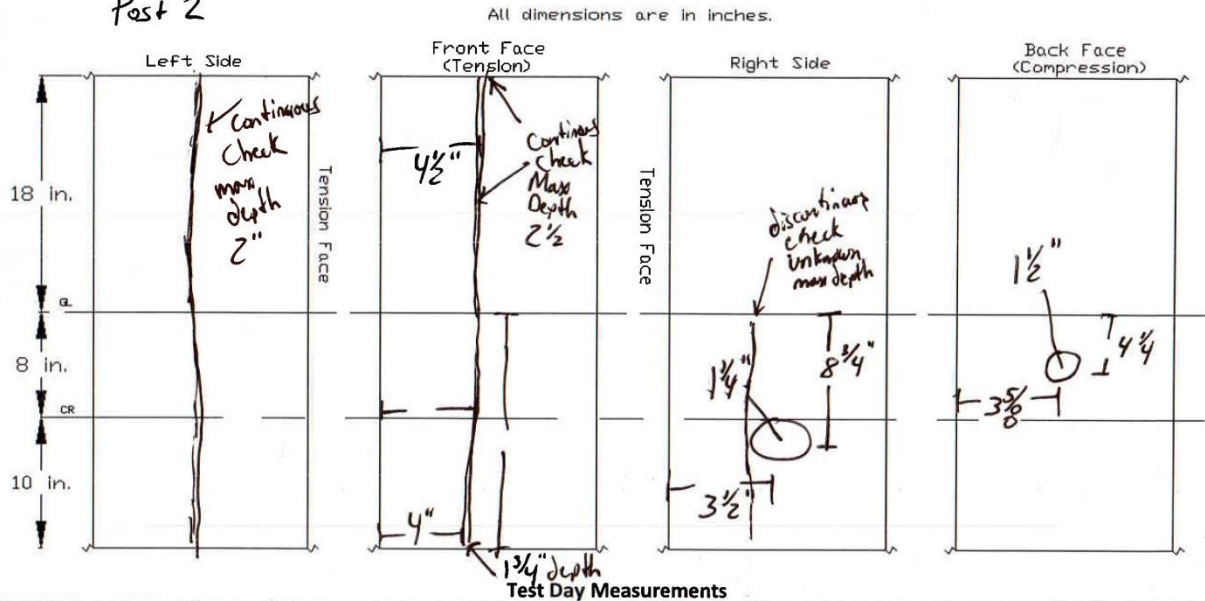
Figure C-1. 6-in. x 8-in. (152-mm x 203-mm) SYP Post Inspection, Test No. SYP W-1

Non-Round Post Inspection/Properties

Rev. 1 (1/4/2014)

Test No.: Post 2

Knot/Defect Inspection Date: 6-17-14



Date Measured: 6-18-14

Post Length: 72 1/8"
 Post Weight: 72 lbs
 Ring Density: 20% = 6 2/3 ring/inch
 Additional Notes:

	Top	GL	CR	Bottom
Width	<u>7 5/8</u>	<u>7 1/4</u>	<u>7 1/4</u>	<u>7 3/8</u>
Depth	<u>5 1/4</u>	<u>5 3/4</u>	<u>5 3/4</u>	<u>5 1/4</u>
Moisture				

67

Figure C-2. 6-in. x 8-in. (152-mm x 203-mm) SYP Post Inspection, Test No. SYP W-2 through SYP W-4

END OF DOCUMENT